Enzymology of Hydrogen Sulfide Turnover

1

Nicole Motl, Pramod Yadav, and Ruma Banerjee

Abstract

Hydrogen sulfide is a biological signaling molecule that is produced by organisms ranging from bacteria to man. Since it is also toxic at high concentrations, strategies exist for its efficient removal and consequent maintenance of low steady-state levels in mammals. Enzymes in the sulfur metabolic network responsible for H_2S biogenesis include the cytoplasmic cystathionine β-synthase and γ-cystathionase enzymes of the transsulfuration pathway as well mercaptopyruvate sulfurtransferase that is both mitochondrial and cytoplasmic. The precursors for H_2S are the amino acids cysteine and homocysteine and a cysteine derivative i.e. mercaptopyruvate. H_2S is cleared via a mitochondrial sulfide oxidation pathway that begins with sulfide quinone oxidoreductase and includes a persulfide dioxygenase, rhodanese and sulfite oxidase. The major oxidation products of H_2S are thiosulfate and sulfate. This chapter focuses on the structural enzymology of H_2S biogenesis and oxidation, emphasizing recent advances in the field.

Keywords

Hydrogen sulfide • Sulfide oxidation • Signaling • Enzymology and regulation

Nicole Motl and Pramod Yadav are equal contributors.

This work was supported in part by the National Institutes of Health (HL58984).

N. Motl • P. Yadav • R. Banerjee (✉)
Department of Biological Chemistry, University of Michigan Medical School, Ann Arbor, MI 48109-0600, USA
e-mail: rbanerje@umich.edu

H. Kimura (ed.), *Hydrogen Sulfide and its Therapeutic Applications*,
DOI 10.1007/978-3-7091-1550-3_1,

Abbreviations

AdoMet	S-adenosylmethionine
CAT	Cysteine aminotransferase
CBS	Cystathionine β-synthase
CSE	γ-cystathionase
ETHE1	Persulfide dioxygenase
H_2S	Hydrogen sulfide
MST	Mercaptopyruvate sulfurtransferase
SQR	Sulfide quinone oxidoreductase

1.1 Introduction to Sulfide Metabolism

Long known as a toxic gas, sulfide like cyanide, targets cellular respiration by reversible inhibition of cytochrome c oxidase. Cells therefore evolved strategies for handling the twin challenges of averting toxicity problems while exploiting the signaling potential of hydrogen sulfide (H_2S), which elicits profound physiological effects (Kimura 2010). Hence, a "safe" window must exist within which low intracellular concentrations of H_2S are maintained and allowed to transiently spike to allow passage of a signal. The concentration width of this window could span three orders of magnitude since steady-state intracellular concentrations of H_2S are estimated to be in the 15–30 nM range (Furne et al. 2008; Levitt et al. 2011; Vitvitsky et al. 2012) while mammalian mitochondrial ATP production is abolished at 50 μM H_2S (Bouillaud and Blachier 2011). The steady-state concentrations of H_2S is a product of both the metabolic flux through the sulfide biogenesis and sulfide oxidation pathways (Vitvitsky et al. 2012) (Fig. 1.1).

Three enzymes in the mammalian sulfur metabolic network catalyze H_2S biogenesis (Kabil and Banerjee 2010; Singh and Banerjee 2011). Two of these enzymes reside in the cytosolic transsulfuration pathway and are cystathionine β-synthase (CBS) and γ-cystathionase (CSE). Both are versatile and catalyze H_2S production in a variety of reactions starting from cysteine and/or homocysteine (Chen et al. 2004; Chiku et al. 2009; Singh et al. 2009). The third enzyme, mercaptopyruvate sulfur transferase (MST) (Nagahara et al. 1998; Shibuya et al. 2009), is both cytosolic and mitochondrial in location and transfers the sulfur atom from mercaptopyruvate to an acceptor from where it can be subsequently released as H_2S. MST works in conjunction with the PLP-dependent enzyme, aspartate/cysteine aminotransferase (CAT), which catalyzes the conversion of cysteine to 3-mercaptopyruvate. Recently, D-amino acid oxidase has been reported to convert D-cysteine to 3-mercaptopyruvate, providing an alternative supply route for the MST substrate (Shibuya et al. 2013).

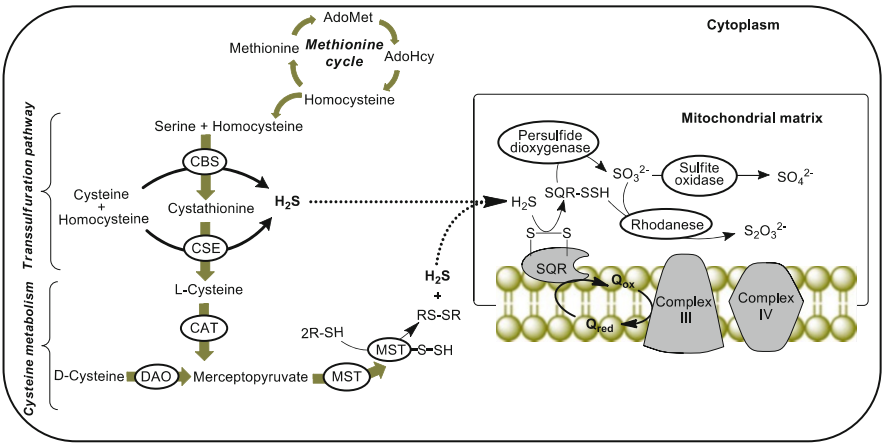

Fig. 1.1 Scheme showing pathways of biogenesis and catabolism of H_2S. DAO is D-amino acid oxidase

Sulfide oxidation occurs in the mitochondria and connects sulfur metabolism to the electron transfer chain and thereby, to both ATP and reactive oxygen species production (Fig.1.1). Half maximal inhibition of cytochrome *c* oxidase in cell extracts occurs at concentrations of ~0.3 μM versus ~20 μM H_2S needed to inhibit cellular respiration in intact cells (Bouillaud and Blachier 2011). To avoid intracellular sulfide build-up and consequent toxicity, the sulfide oxidation pathway is activated at considerably lower (~10–20 nM) sulfide concentrations (Bouillaud and Blachier 2011). The high sensitivity of the sulfide oxidation pathway to H_2S, suggests that the duration of H_2S-based signaling is likely to be short (Bouillaud and Blachier 2011). Sulfate and thiosulfate are the major products of the mammalian mitochondrial sulfide oxidation pathway, which comprises four enzymes: sulfide quinone oxidoreductase (SQR), a persulfide dioxygenase (ETHE1) that is the product of the *ethe1* gene, rhodanese, and sulfite oxidase (Hildebrandt and Grieshaber 2008). This chapter focuses on the structural enzymology and regulation of H_2S metabolism.

1.1.1 Enzymology of H_2S Biogenesis

1.1.1.1 Cystathionine β-Synthase

Structural Organization of CBS. CBS is a multidomainal protein, which in its role in the transsulfuration pathway, catalyzes the condensation of homocysteine and serine to produce cystathionine (Banerjee et al. 2003). Homocysteine is a redox-active nonprotein amino acid that is produced by hydrolysis of S-adenosylhomocysteine, a product of S-adenosylmethionine (AdoMet)-dependent methylation reactions. Homocysteine is either recycled in the methionine cycle via the action of methionine synthase or committed to cysteine synthesis by the action of CBS (Fig. 1.1).

Mutations in CBS are the most common cause of homocystinuria, an autosomal recessive disorder, characterized by severely elevated plasma homocysteine levels (Kraus et al. 1999). CBS deficiency affects multiple organ systems including the ocular, skeletal, cardiovascular and the central nervous system (Mudd et al. 1964).

In addition to the canonical transsulfuration reaction, CBS catalyzes H_2S-producing reactions in which serine is substituted by cysteine (Chen et al. 2004; Singh et al. 2009). These reactions involve β-replacement of cysteine by homocysteine, cysteine or water to generate cystathionine, lanthionine or serine, respectively in addition to the common product, H_2S.

CBS is a homodimeric enzyme. The full-length human enzyme is prone to aggregation and exists in multiple oligomeric states ranging from 2- to 16-mers (Sen and Banerjee 2007). The predominance of the 4-mer in the aggregated mixture has led to confusion in the literature about CBS being a homotetramer. Each monomer is organized into an N-terminal heme-binding domain, a central PLP-binding catalytic core and a C-terminal AdoMet-binding regulatory domain, which contains a tandem repeat of CBS domains. The latter, named after this protein, is found in all three domains of life and refers to a $\beta-\alpha-\beta-\beta-\alpha$ secondary structure motif often associated with energy sensing that binds ATP or AMP (Bateman 1997). In CBS, it binds the allosteric activator, AdoMet, which renders transsulfuration flux sensitive to cellular methyl donor status. Thus, when AdoMet levels are low, sulfur is spared and utilized via the methionine cycle to support AdoMet synthesis. In contrast, when AdoMet levels are plentiful, sulfur metabolism is directed towards cysteine synthesis via activation of CBS.

The crystal structures of full-length CBS from *Drosophila melanogaster* (dCBS, Fig. 1.2a) and a truncated variant of human CBS (hCBS) lacking the C-terminal regulatory domain have been reported (Meier et al. 2001; Taoka et al. 2002; Koutmos et al. 2010). The N terminal heme domain spans residues 1–70 in hCBS and 1–45 in dCBS while the middle PLP domain spans residues 71–411 in hCBS and 46–350 in dCBS. A 27 residue-long linker (351–377) visible in the structure of dCBS connects the PLP and C-terminal domains, which based on sequence alignment, is predicted to extend between residues 382–411 in hCBS.

Catalytic Mechanism of CBS. The active site of CBS is lined with residues that position the substrates and cofactor for catalysis. PLP is covalently linked to an active site lysine (K119 in hCBS and K88 in dCBS) and its phosphate moiety is enveloped by a glycine-rich loop (T_{260}-G_{259}-G_{258}-T_{257}-G_{256}, hCBS numbering) (Fig. 1.2b). N149 and S349 form hydrogen bonds with the exocyclic oxygen and pyridine nitrogen, respectively (Meier et al. 2001; Taoka et al. 2002). Replacement of the corresponding serine in yeast CBS (yCBS) by alanine results in complete loss of activity, while replacement with aspartate results in an ~80-fold lower activity despite the mutants having only two-fold lower PLP occupancy (Quazi and Aitken 2009). Fluorescence and resonance Raman studies demonstrate that the PLP exists in two tautomeric forms: an active ketoenamine and an inactive enolimine (Singh et al. 2009; Weeks et al. 2009; Yadav et al. 2012). N149 helps stabilize the active ketoenamine tautomer. Perturbations in the hydrogen-bonding network in the active site can influence the tautomeric equilibrium, and as described below, is

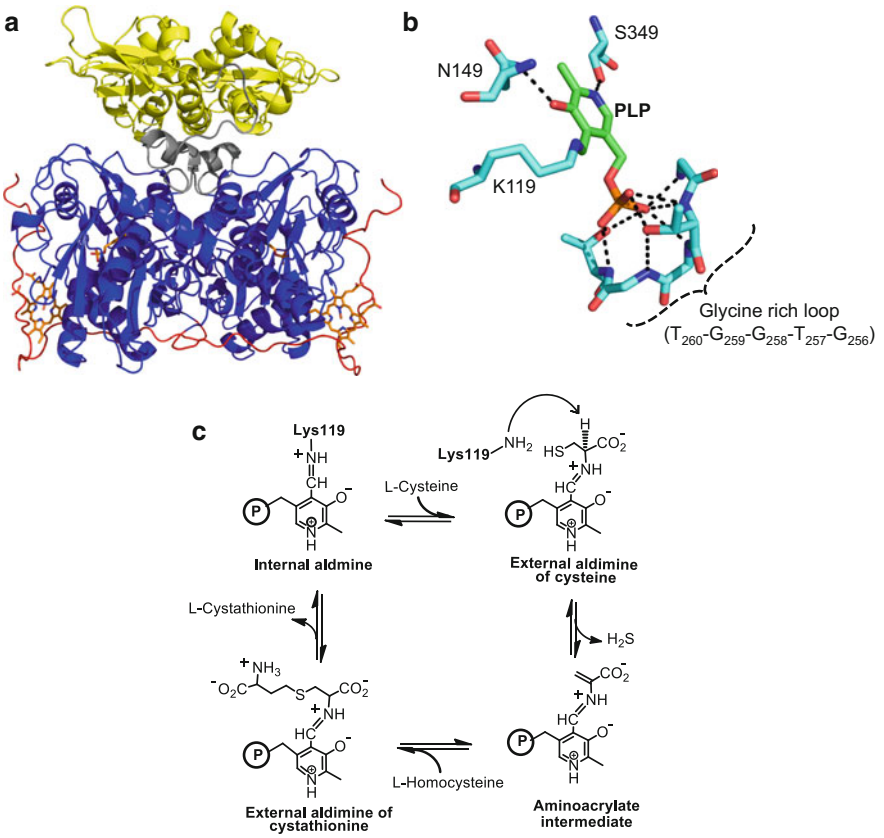

Fig. 1.2 Structure and catalytic mechanism of CBS. (**a**) Structure of full-length dCBS. The protein comprises an N-terminal heme-binding domain (*red*), a PLP domain (*blue*) and a C-terminal AdoMet-binding domain (*yellow*). A linker (*grey*) connects the PLP- and C-terminal domains. (**b**) Close-up of the active site of hCBS. Hydrogen bonds between PLP and amino acids lining the active site are shown as *dotted lines*. Figure 1.2a, b were generated using PDB files 3PC2 and 1 M54, respectively. (**c**) Proposed catalytic mechanism for H_2S generation from cysteine by CBS. The resting enzyme exists as an internal aldimine, which reacts with cysteine to form the external aldimine of cysteine. Elimination of H_2S leads to formation of an aminoacrylate intermediate, which reacts with homocysteine (cysteine or water) to form the external aldimine of the product cystathionine (or lanthionine or serine). The catalytic cycle is completed upon release of product and reformation of internal aldimine

one mechanism by which the heme cofactor exerts its effects on the active site (Singh et al. 2009; Yadav et al. 2012).

The first step in the catalytic cycle (Fig. 1.2c) is binding of serine or cysteine (Fig. 1.2c) to the active site followed by displacement of the lysine residue that forms an internal aldimine with PLP (Banerjee et al. 2003). Abstraction of the α-proton from the resulting external aldimine of serine/cysteine generates a carbanion intermediate. In the crystal structure of dCBS obtained at 1.7 Å resolution, the

carbanion intermediate with serine was captured and revealed how the active site stabilizes this reactive species (Koutmos et al. 2010). The Cα atom is clearly sp^2 hybridized in this intermediate and the ε-amino group of K88 is within 2.1, 2.5 and 3.0 Å of the Cα, imino nitrogen of the Schiff base and C4A of PLP, respectively, where the negative charge is predominantly localized. Elimination of H_2O or H_2S from the external aldimine of serine or cysteine, respectively leads to formation of the aminoacrylate intermediate, which was also captured in a crystal structure of dCBS obtained at 1.55 Å resolution (Koutmos et al. 2010). In this structure, the Cα is also clearly sp^2 hybridized and the ε-amino group of K88, which is swung away from Cα, is parked near the oxygen atoms of the phosphate moiety of PLP. The Cβ of the aminoacrylate intermediate is positioned for nucleophilic attack by the thiolate of homocysteine (to generate cystathionine), or cysteine (to generate lanthionine) or by water (to generate serine). The final step preceding product release involves a second transchiffization reaction in which the active site lysine displaces the product and the enzyme returns to its resting internal aldimine state.

Kinetics of H_2S Generation by CBS. Detailed steady-state kinetic analyses of H_2S generation by human and yeast CBS have been reported (Singh et al. 2009). In addition to the canonical β-replacement reaction in the transsulfuration pathway (Eq. 1.1), CBS catalyzes at least three other reactions with a combination of cysteine and homocysteine as substrates, leading to H_2S production (Eqs. 1.2, 1.3, and 1.4). The CBS active site has two pockets for binding amino acids that

$$\text{Serine} + \text{Homocysteine} \rightarrow \text{Cystathionine} + H_2O \tag{1.1}$$

$$\text{Cysteine} + \text{Homocysteine} \rightarrow \text{Cystathionine} + H_2S \tag{1.2}$$

$$\text{Cysteine} \rightarrow \text{Serine} + H_2S \tag{1.3}$$

$$\text{Cysteine} + \text{Cysteine} \rightarrow \text{Lanthionine} + H_2S \tag{1.4}$$

are designated as sites 1 and 2. Site 1 binds the amino acid that forms the external aldimine with PLP while site 2, binds the nucleophilic amino acid (Singh et al. 2009). At saturating substrate concentrations, the specific activity for the β-replacement of cysteine by homocysteine (reaction 2) is ~4-fold higher than for the canonical β-replacement of serine by homocysteine (reaction 1). H_2S generation from one (reaction 3) or two (reaction 4) moles of cysteine results in serine or lanthionine and are ~40- and ~20-fold lower, respectively than H_2S generation from cysteine and homocysteine (Singh et al. 2009).

Within the cell, the efficiency of each CBS-catalyzed reaction is dictated in part by the relative concentrations of the individual substrates and the K_M values, which are high for both yeast and human CBS relative to the intracellular concentrations of their amino acid substrates. The K_M for cysteine for hCBS at site 1 is 6.8 ± 1.7 mM and higher still for site 2 (27.3 ± 3.7 mM). For yCBS, the K_M values for cysteine at sites 1 and 2 are 3.6 ± 1.7 mM and 33 ± 3.7 mM, respectively. Homocysteine only binds to site 2 and the K_Ms for yeast and human CBS are 0.13 ± 0.02 mM and

3.2 ± 1.3 mM, respectively (Singh et al. 2009). Simulations were performed using the steady-state kinetic data for hCBS at physiological concentrations of substrate (560 μM serine, 100 μM cysteine and 10 μM homocysteine). The simulations predicted that ~96 % of H_2S derived from hCBS is via β-replacement of cysteine by homocysteine with the remainder being contributed by the other two reactions (Singh et al. 2009).

Pre-steady state kinetic analysis and characterization of reaction intermediates was first reported for yCBS using stopped flow spectroscopy (Jhee et al. 2001; Taoka and Banerjee 2002; Singh et al. 2011). The heme in hCBS interferes with enzyme-monitored pre-steady state kinetic analysis by masking the PLP absorbance. Kinetic analysis of a heme-less hCBS variant lacking the N-terminal heme domain was limited by its poor stability (Evande et al. 2004). We have recently employed difference UV-visible stopped-flow spectroscopy to characterize intermediates in the hCBS-catalyzed reaction (Yadav and Banerjee 2012), an approach, that we used previously to demonstrate the intermediacy of an aminoacrylate intermediate in dCBS (Koutmos et al. 2010). The rate of aminoacrylate formation is ~2.5-fold faster with serine than with cysteine in the reaction catalyzed by hCBS and product release appears to limit the overall reaction rate (Yadav and Banerjee 2012).

Allosteric Regulation of CBS by Heme. The N-terminal heme domain in CBS is devoid of any secondary structure. The heme is hexa-coordinate and its histidine and cysteine axial ligands were predicted by EPR, extended X-ray absorption fine structure (Ojha et al. 2000) and resonance Raman (Green et al. 2001) spectroscopy. The UV-visible spectrum of ferric CBS exhibits a Soret peak at 428 nm and a broad α/β absorption band centered at 550 nm. In the ferrous state, the Soret peak shifts to 449 nm with concomitant sharpening of the α and β absorption bands at 571 and 540 nm (Taoka et al. 1998). Mutation of either heme ligand diminishes hCBS activity (by ~9-fold) despite full PLP saturation in the C52A and C52S mutants and 75 % saturation in the H65R mutant (Ojha et al. 2002). On the other hand, heme saturation is greatly reduced in the heme ligand mutants (19 % and 40 % in the cysteine and histidine ligand mutants, respectively) compared to wild-type CBS. The C52S or C52A mutants have five-coordinate high-spin heme with a Soret peak blue-shifted from 428 to 415–417 nm in the ferric form and from 449 to 423 nm in the ferrous form (Ojha et al. 2002). In the ferrous-CO state, the Soret peaks of the mutants (at ~422 nm) are virtually identical to that of wild-type enzyme, consistent with the substitution of the cysteine ligand by CO. The Soret peaks in the ferric, ferrous and ferrous-CO states in the H65R mutant are at 424, 421 and 420 nm, respectively, consistent with the presence of a low-spin heme (Ojha et al. 2002).

While the role of the heme domain in CBS has been debated, there is growing evidence that it regulates CBS activity in response to changes in the heme spin-or ligation-state (Taoka and Banerjee 2001; Taoka et al. 2001; Singh et al. 2007). The ferrous heme ligands CO and NO, inhibit CBS activity (Taoka et al. 1999; Taoka and Banerjee 2001). Ferrous-NO CBS is five-coordinate with a broad Soret peak at ~390 nm (Taoka and Banerjee 2001). CBS exhibits nonequivalent binding sites for CO with K_d values of 1.5 ± 0.1 μM and 68 ±14 μM for full-length hCBS and

3.9 ± 2 μM and 50 ± 8 μM for the C-terminal truncated form (Taoka et al. 1999; Puranik et al. 2006). Binding of NO to full-length CBS exhibits a K_d of 30 ± 5 μM for NO (Gherasim et al., unpublished results). Binding of CO to full-length CBS inhibits enzyme activity with a K_i value of 5.6 ± 1.9 μM (Taoka et al. 1999). The redox potential of the heme is −350 ± 4 mV (Singh et al. 2009) and −287 ± 2 mV (Carballal et al. 2008) in full-length and truncated hCBS, respectively. This difference between the full-length and truncated forms suggests that the regulatory C-terminal domain modulates the heme redox potential. We have recently demonstrated that despite the low reduction potential of the CBS heme, reversible regulation by CO can be achieved with physiologically relevant reductants (Kabil et al. 2011). The diflavin oxidoreductases, human methionine synthase reductase and novel reductase 1 reduce ferric CBS and the ferrous-CO species is formed in the presence of NADPH and CO.

Communication between the heme and PLP domains occurs via an α-helix whose N-terminal end leads in from the glycine rich loop harboring the conserved T257 and T260 residues that make contact with the phosphate moiety of PLP. At the C-terminal end of the helix, R266 is involved in a salt-bridge interaction with the heme ligand, C52. Changes in the heme coordination state e.g. by formation of the ferrous-CO species, is predicted to disrupt the salt bridge between C52 and R266, displacing the α-helix, which in turn is propagated to the PLP site shifting the tautomeric equilibrium towards the enolimine (Weeks et al. 2009). Interestingly, replacement of R266 by methionine, a mutation described in homocystinuric patients, also results in the predominance of the inactive enolimine. Similarly, substitutions at T257 and T260 in the PLP domain, stabilize the inactive enolimine tautomer leading to significant loss of CBS activity (Yadav et al. 2012). Interestingly, these CBS mutations impact the H_2S and cystathionine-producing versus H_2O and cystathionine-producing reactions unequally, suggesting that that these two activities can be differentially regulated (Yadav et al. 2012).

Allosteric Regulation of CBS by AdoMet. AdoMet binds to the C-terminal regulatory domain (Scott et al. 2004) and enhances CBS activity ~2–3-fold (Finkelstein et al. 1975). Truncation of the C-terminal domain in hCBS leads to loss of AdoMet-dependent regulation, increases CBS activity and also decreases its propensity for aggregation (Kery et al. 1998). Hence, the regulatory domain exerts an autoinhibitory effect that is alleviated upon AdoMet binding, activating mutations or deletion of the entire domain (Shan and Kruger 1998; Janosik et al. 2001; Evande et al. 2002). The architecture of the regulatory domain and its juxtaposition relative to the catalytic domain was first visualized in the structure of full-length dCBS (Fig. 1.2a). The secondary structures of the two CBS domains are slightly different: β-α-β-β-α-α-β fold in one (spanning residues 416–468 in hCBS) and α-β-α-β-β-α in the second (residues 486–543). The AdoMet binding sites in CBS is predicted to reside in the β-sheet-lined cleft between the two CBS domains.

Other Mechanisms for Regulation of CBS Activity. As a junction enzyme in sulfur metabolism, CBS is the locus of complex regulation. AdoMet is an allosteric regulator, which activates CBS under conditions of methyl group sufficiency (Prudova et al. 2006; Pey et al. 2013). As noted above, gaseous signaling molecules

like NO and CO bind to the heme in CBS and inhibits its activity (Taoka et al. 1999; Taoka and Banerjee 2001; Agarwal and Banerjee 2008; Yamamoto et al. 2011; Yadav et al. 2012), which is reversed upon air oxidation (Kabil et al. 2011b). Sumoylation of CBS decreases its activity (Agarwal and Banerjee 2008). K211 in the catalytic core of human CBS appears to be the site of sumoylation. In addition, the C-terminal regulatory domain of CBS is needed for sumoylation. CBS is reportedly inhibited by lanthionine synthase C-like protein 1 (LanCL1) in the presence of glutathione (Zhong et al. 2012). Under oxidative stress conditions, when oxidized glutathione levels rise, inhibition by LanCL1 is alleviated providing a mechanism for increasing transsulfuration flux and consequently, glutathione synthesis.

1.1.1.2 Cystathionine γ Lyase

Structural Organization of CSE. Human CSE (hCSE) is a homotetrameric enzyme that catalyzes the second step in the transulfuration pathway cleaving cystathionine to cysteine, α-ketobutyrate, and ammonia (Fig. 1.3a). The crystal structures of yeast (yCSE) and hCSE are available at 2.6 Å resolution each (Messerschmidt et al. 2003; Sun et al. 2009). Each hCSE monomer comprises a large N-terminal PLP-binding domain (residues 1–263) and a smaller C-terminal domain (residues 264–401) (Fig. 1.3a). The yCSE monomer comprises three domains: an N-terminal domain, which interacts with the active site of a neighboring monomer, a middle catalytic domain and a small C-terminal domain. The yCSE catalytic and C-terminal domains are organized as in hCSE while the N-terminal extension interacts with the active site of the neighboring subunit, is not present in hCSE and comprises an extended loop, an α-helix and a β-strand (Messerschmidt et al. 2003).

Mutations in CSE, inherited as an autosomal recessive disorder, results in cystathioninuria, which is often benign (Wang and Hegele 2003). Cystathioninuria can be secondarily associated with hepatoblastoma, neuroblastoma, poor development, cystic fibrosis and Down's syndrome.

Catalytic Mechanism of CSE. Like CBS, CSE also catalyze various reactions leading to H_2S biogenesis in addition to catalyzing the canonical reaction in the transsulfuration pathway (Chiku et al. 2009; Singh et al. 2009). The PLP is covalently linked to K212 in hCSE via a Schiff base and its mutation to alanine reduces H_2S production ~80-fold compared to wild-type enzyme. Several active site residues are engaged in hydrogen bonding interactions with the PLP (Messerschmidt et al. 2003; Sun et al. 2009); N187 with the pyridine nitrogen and G90, L91, S209 and T211 from one subunit and Y60 and R62 from an adjacent subunit with the phosphate moiety (Fig. 1.3b). Replacement of N187 with alanine or glutamic acid results in complete loss of H_2S production while substitutions of S209 and T211 by alanine result in a modest ~1.5-fold decrease in H_2S production (Huang et al. 2010). Interactions between Y60 and R62 contributed by the N-terminal domain of a neighboring monomer and the phosphate group of PLP helps to stabilize the active site, which is located at the interface between adjacent subunits. Multiple sequence alignment of human,

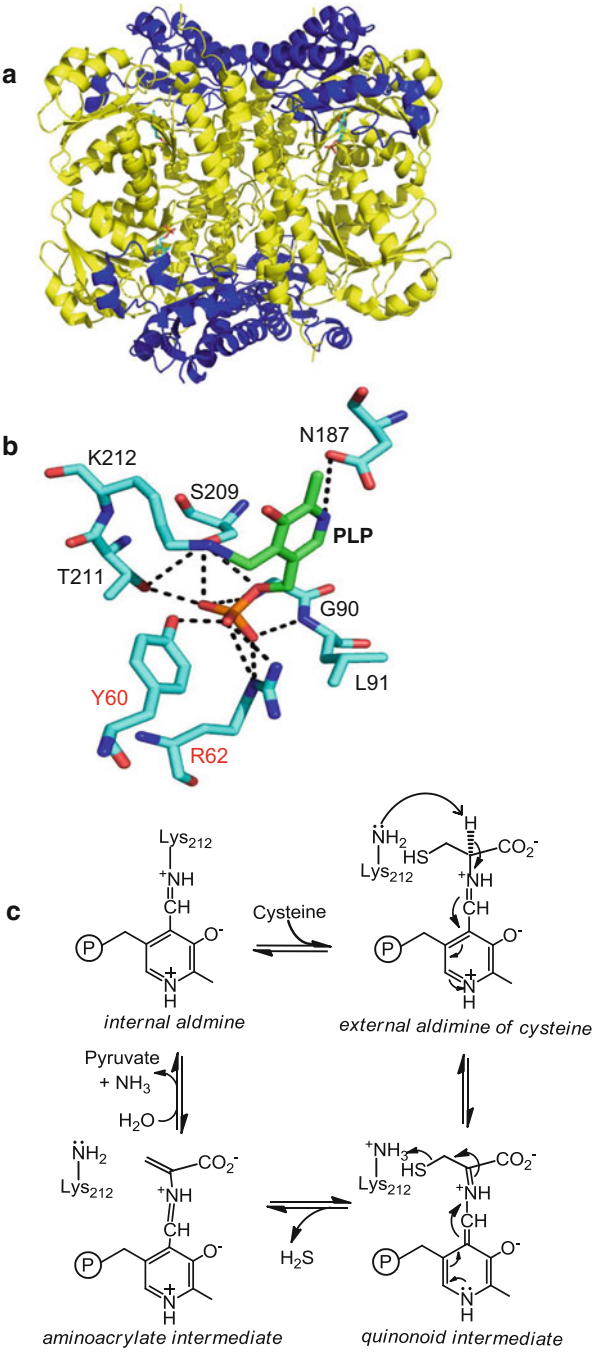

Fig. 1.3 Structure and catalytic mechanism of CSE. (**a**) Structures of tetrameric hCSE comprising an N-terminal catalytic domain (*yellow*) and a C-terminal domain (*blue*). PLP is shown in stick representation (*cyan*). (**b**) Close-up of the active site of hCSE. Hydrogen bonds between PLP and amino acids lining the active site are shown as *dotted lines*. The *red labels* denote residues contributed by a neighboring subunit. Figure 1.3a, b were generated using PDB file 2NMP. (**c**) Proposed catalytic cycle of CSE for H_2S generation. Cysteine reacts with the resting enzyme and forms external aldimine of cysteine. Abstraction of the α-proton of bound cysteine leads to formation of cysteine-ketamine intermediate. Cleavage of the C–β–S bond eliminates H_2S and leads to formation of the aminoacrylate intermediate, which undergoes hydrolysis to give pyruvate and ammonia. In the final step, free PLP rebinds with the K212 to regenerate the resting internal aldimine

yeast, mouse, rat and slime mold CSEs reveals that Y60 and R62 are conserved in all five sequences (Huang et al. 2010). Substitution of Y60 with threonine or alanine results in an ~5–8-fold decrease in hCSE activity, while replacement of R62 with alanine or lysine results in an ~10–36-fold decrease in activity (Huang et al. 2010).

CSE belongs to the γ-family of PLP-dependent enzymes, which catalyze elimination reactions at the γ-carbon. However, in the case of CSE, the specificity is not high and the enzyme catalyzes reactions at both the β- and γ-carbons of the substrate. In the first step, the substrate (i.e. cystathionine or cysteine) forms a Schiff base with the PLP via a transaldimination reaction, freeing the active site K212 residue. In the next step, K212 presumably acts as the general base and abstracts the α-proton from bound substrate. When cystathionine is the substrate, cleavage of the C-γ-S bond is promoted by a second proton abstraction from Cβ resulting in the subsequent elimination of cysteine. Hydrolysis of the resulting imine intermediate yields α-ketobutyrate and ammonia. Alternatively, when cysteine is the substrate, the C-β-S bond is cleaved, releasing H_2S (Fig. 1.3c). A second transaldimination reaction regenerates the resting internal aldimine. UV-visible spectroscopy based pre-steady state kinetic analysis of the reaction catalyzed by yCSE suggests that product release constitutes the rate-limiting step (Yamagata et al. 2003).

The specificity of the hCSE-catalyzed α,γ-elimination versus α,β-elimination is proposed to be governed by the hydrophobicity of the residue at position 339 (Messerschmidt et al. 2003; Huang et al. 2010). This hypothesis was tested by replacing E339 with lysine, alanine and tyrosine, which increases hydrophobicity in the following order: Y>A>K>E. E339K, E339A and E339Y show approximately 1.8-, 3.2- and 7.2-fold increase, respectively in the catalytic efficiency of H_2S production from cysteine as compared to wild-type enzyme (Huang et al. 2010), consistent with the view that enhancing the hydrophobicity of the residue at position 339 in hCSE favors the α,β-elimination reaction.

Kinetics of H_2S Generation by CSE. Detailed steady-state kinetic analysis of hCSE revealed that in addition to the canonical cystathionine cleavage reaction in the transsulfuration pathway (Eq. 1.5), the enzyme can catalyze five distinct H_2S-generating reactions in the presence of cysteine and/or homocysteine (Eqs. 1.6, 1.7, 1.8, 1.9, and 1.10) (Chiku et al. 2009).

$$\text{L-Cystathionine} + H_2O \rightarrow \text{L-cysteine} + \alpha\text{-Ketobutyrate} + NH_3 \quad (1.5)$$

$$\text{L-Cysteine} + H_2O \rightarrow \text{L-Pyruvate} + NH_3 + H_2S \quad (1.6)$$

$$\text{L-Cysteine} + \text{L-Cysteine} \rightarrow \text{L-Lanthionine} + H_2S \quad (1.7)$$

$$\text{L-Homocysteine} + H_2O \rightarrow \text{L-Homoserine} + H_2S \quad (1.8)$$

$$\text{L-Homocysteine} + \text{L-Homocysteine} \rightarrow \text{L-Homolanthionine} + H_2S \quad (1.9)$$

$$\text{L-Homocysteine} + \text{Cysteine} \rightarrow \text{L-cystathionine} + H_2S \quad (1.10)$$

Unlike hCSE (Chiku et al. 2009), rat CSE reportedly utilizes cystine, the oxidized disulfide form of cysteine, as a substrate for H_2S production (Stipanuk and Beck 1982). However, the availability of cystine in the reducing cellular milieu is questionable and the immediate product of the reaction is cysteine persulfide, which is highly unstable. Under maximal velocity conditions, the highest rate of H_2S production is observed for reaction 1.9, i.e. γ-replacement of homocysteine by a second mole of homocysteine while the lowest rate is observed for reaction 1.6, i.e. α,β−elimination of cysteine (Chiku et al. 2009). At physiological substrate concentrations, the highest rate of H_2S production is predicted to occur via the α,β−elimination reaction of cysteine and the lowest rate from the β−replacement of cysteine by a second mole of cysteine (reaction 1.7).

CSE exhibits two substrate-binding sites: site 1 at which the Schiff base is formed between PLP and an amino acid and site 2 where the nucleophilic second amino acid binds. The K_M for cysteine at site 1 (1.7 ± 0.7 mM) is ~1.6-fold lower than for homocysteine (2.7 ± 0.8 mM) while for the K_M for homocysteine at site 2 (5.9 ± 1.2 mM) is ~6-fold lower than for cysteine (33 ± 8 mM). The lower K_M for cysteine versus homocysteine at site 1 together with the higher cellular concentration of cysteine (~100 μM) versus homocysteine (<10 μM), explains the predominance of reaction 1.6 versus 1.9 at physiologically relevant substrate concentrations (Chiku et al. 2009).

The relative contributions of the various CSE-catalyzed H_2S producing reactions has been estimated at physiologically relevant substrate concentrations (5 μM cystathionine, 100 μM cysteine and 10 μM homocysteine) and low (10 μM), moderate (40 μM) and severe (100 μM) hyperhomocysteinemia (Chiku et al. 2009). Simulations predict that under normal and hyperhomocysteinemic conditions, ~87–99.5 % of the total H_2S is derived via α,β-elimination of cysteine and α,γ-elimination reaction of homocysteine, while the remaining three reactions collectively contribute very little. Between the two major H_2S contributing reactions, the α,β-elimination of cysteine predominates (~71 %) at normal homocysteine concentrations while the α,γ-elimination of homocysteine is the major H_2S producer accounting for ~61 % and ~78 % H_2S, respectively under moderate and severe hyperhomocysteinemic conditions (Chiku et al. 2009).

Preliminary pre-steady state kinetic analyses of the yCSE-catalyzed reaction were performed at 5 °C and 30 °C (Yamagata et al. 2003). An aminocrotonate intermediate was detected ($\lambda_{max} = 480$ nm) upon rapid mixing of yCSE with cystathionine but not with L-cysteine. Conversion of the aminocrotonate intermediate to products represents the rate-limiting step in the CSE-catalyzed cleavage of csytathionine (Yamagata et al. 2003).

Regulation of CSE. Unlike CBS, mechanisms for regulating CSE activity are not well understood. H_2S formation by CSE was reported to be upregulated by calmodulin in the presence of 2 mM Ca^{2+} (Yang et al. 2008). However, Ca^{2+}/calmodulin-dependent regulation of purified hCSE has not been observed in our laboratory (Padovani and Banerjee, unpublished results). A recent study on rat CSE supports our observations (Mikami et al. 2013) since the rate of H_2S production was low in the presence of 2 mM cysteine and 0–100 nM Ca^{2+} and increased five-fold when 50 μM PLP was added to the reaction mixture. At higher Ca^{2+} concentrations (0.3–3.0 μM), the rate of H_2S production was ~2.5-fold lower in the presence or absence of PLP compared to that at lower Ca^{2+} concentrations (less than 0.3 μM). Calmodulin (1 μM) had no effect on H_2S production by CSE. These findings suggest that CSE is not regulated by calmodulin and that low Ca^{2+} enhances H_2S production but only in the presence of exogenous PLP while high Ca^{2+} concentrations (300 nM to 3 μM) inhibit CSE (Mikami et al. 2013). While CSE can be sumoylated in vitro (Agarwal and Banerjee 2008), the physiological relevance of this modification is not known. Mammalian CSE has two conserved CXXC motifs. However, their involvement in redox-dependent regulation of CSE activity is not known.

1.1.1.3 Mercaptopyruvate Sulfurtransferase

Structural Organization of MST. MST functions on a catabolic arm of cysteine metabolism and acts downstream of CAT to produce H_2S (Meister et al. 1954; Stipanuk and Beck 1982). CAT, which is identical to aspartate aminotransferase, catalyzes the conversion of cysteine in the presence of α-ketoglutarate to 3-mercaptopyruvate and ammonia. 3-Mercaptopyruvate is a substrate for MST, which transfers the sulfur group to a catalytic cysteine residue forming an enzyme-bound persulfide and releasing pyruvate. In the second half reaction, the sulfane sulfur is transferred to a thiol acceptor e.g. cysteine, homocysteine, dihydrolipoic acid, GSH or thioredoxin and subsequently released as H_2S (Nagahara et al. 2007; Mikami et al. 2011a; Yadav et al. 2013). The MST-bound persulfide can also be transferred to non-thiol acceptors like KCN to form thiocyanate (Nagahara et al. 1999). Recently an alternative to the transamination pathway has been reported for the production of 3-mercaptopyruvate from D-cysteine in a reaction catalyzed by D-amino acid oxidase (Shibuya et al. 2013). The latter, is expressed in multiple tissues and is most abundant in the cerebellum and kidney (Shibuya et al. 2013). Defects in the MST gene are inherited as an autosomal recessive disorder known as mercaptolactate-cysteine disulfiduria (Crawhall et al. 1968). The condition is characterized by excessive excretion of mercaptolactate-cysteine disulfide in the urine, with or without mental retardation. Mercaptopyruvate is oxidized by lactate dehydrogenase to mercaptolactate and reacts subsequent to export, with extracellular cysteine to form the mixed disulfide of mercaptolactate and cysteine (Nagahara and Sawada 2006).

The crystal structures of MST from *E. coli* and *Leishmania major* have been solved at 2.8 Å and 2.1 Å resolution, respectively (Alphey et al. 2003; Spallarossa et al. 2004). Recently, our laboratory has obtained the structure of the product

complex of hMST at 2.15 Å resolution with pyruvate and persulfide bound at the active site (Yadav et al. 2013). Both bacterial and human MST comprise two domains connected by a linker, which are structurally similar to the rhodanese domain (Fig. 1.4a). The *Leishmania* MST has an extra ~80 amino acids long domain that shares structural homology with the immunosuppressant FK506-binding protein and to macrophage infectivity potentiator protein, both of which exhibit peptidyl prolyl cis-trans isomerase activity (Alphey et al. 2003). Expression of a C-terminally truncated *Leishmania* MST yields a misfolded protein devoid of catalytic activity (Williams et al. 2003). The C-terminal domain in the *L. major* MST is postulated to be involved in protein folding and protein–protein interactions (Alphey et al. 2003).

Catalytic Mechanism of MST. A conserved cysteine residue (C248 in hMST) plays a key role in the catalytic mechanism of this enzyme (Fig. 1.4b). All three available MST structures exhibit persulfides at the active site cysteine residue, which represents the product of the MST-catalyzed sulfur transfer from 3-mercaptopyruvate. Substitution of the corresponding active site cysteine with serine in rat MST (rMST), results in complete loss of activity (Nagahara and Nishino 1996). Two conserved arginine residues (R188 and R197 in hMST) (Fig. 1.4b) are proposed to be important for proper positioning of the substrate and their replacement with glycine is deleterious for rMST activity. The R187G and R196G mutations increase K_M for 3-mercaptopyruvate by 10- and 60-fold, respectively and decrease k_{cat} 4- and 870-fold, respectively. Based on the *Leishmania* MST crystal structure, a serine protease-like catalytic triad, comprising Ser255-His75-Asp61 was predicted to be a common feature of the MST family. The catalytic triad is proposed to play a role in polarizing the carbonyl bond in the substrate to assist in the nucleophilic attack by the active site cysteine (Alphey et al. 2003). The crystal structure of hMST confirms the presence of a serine protease-like catalytic triad (S250-H74-D63) in the active site (Yadav et al. 2013).

Enzymes belonging to the sulfurtransferase family catalyze the transfer of a sulfur atom from a sulfur donor to a nucleophilic acceptor. Based on steady-state kinetic analysis of bovine MST, the enzyme was proposed to use a sequential mechanism (Jarabak and Westley 1978). Based on the structure of hMST containing a mixture of the product complex (Cys248-SSH and pyruvate) and an unproductive intermediate (3-mercaptopyruvate in a disulfide linkage with Cys248), we have proposed a detailed reaction mechanism (Fig. 1.4c) (Yadav et al. 2013). The conserved arginine residues, R188 and R197, interact via hydrogen bonds with the carboxyl group of mercaptopyruvate while R197 also hydrogen bonds with the carbonyl group of the substrate. H74 in the catalytic triad is proposed to function as a general base, abstracting a proton from S250, which in turn deprotonates C248 for subsequent attack on the sulfur of 3-mercaptopyruvate, leading to transfer of the sulfur atom to form Cys248-persulfide and pyruvate. Following release of pyruvate, an acceptor molecule (e.g. a dithiol or thioredoxin) attacks the sulfane sulfur of the cysteine persulfide regenerating MST and forming a new persulfide on the acceptor. Nucleophilic attack by the second (or resolving cysteine) on the acceptor releases

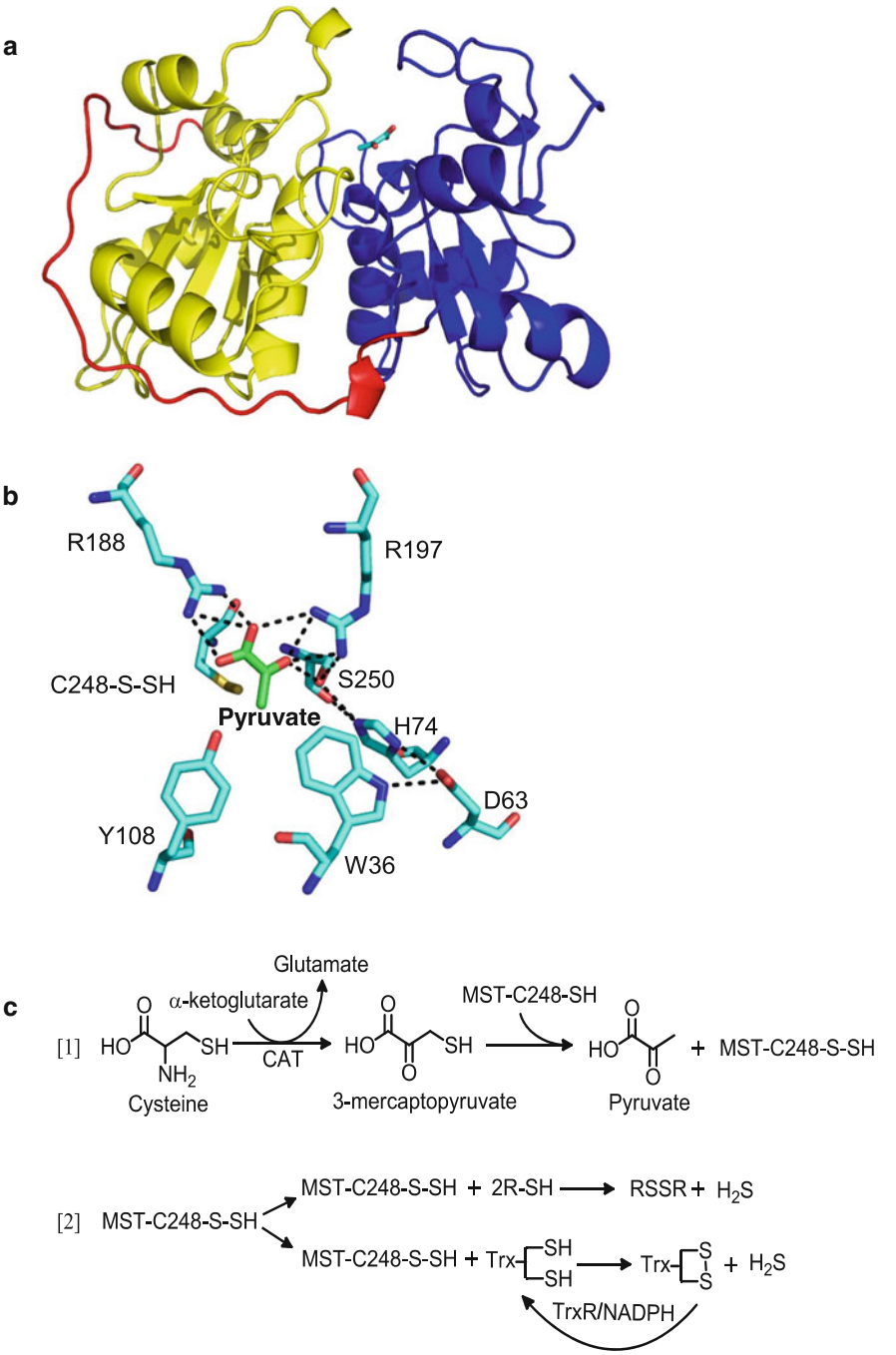

Fig. 1.4 Structure and catalytic mechanism of MST. (**a**) Structure of human MST, which comprises an N-terminal domain (*yellow*) connected to the catalytic domain (*blue*) by a linker (*red*). (**b**) Close-up of the active site of hMST showing a bound persulfide on Cys248 and pyruvate (hydrogen bonds are represented by *dotted lines*). Figure 1.4a, b were generated using PDB file

H_2S and results in oxidized disulfide product. Sulfur transfer from mercaptopyruvate to cyanide generates thiocyanate and pyruvate (Nagahara et al. 1999).

Dihydrolipic acid, thioredoxin, cysteine, homocysteine and glutathione function as acceptors in the in vitro MST assay and a detailed steady state kinetics analysis of H_2S production by MST in the presence of these acceptors have been reported (Yadav et al. 2013). At pH 7.4 and 37 °C kinetic studies revealed that, in the presence of thioredoxin or DHLA, hMST exhibits the highest k_{cat}/K_M values are obtained in the presence of human thioredoxin (520,000 M^{-1} s^{-1}) and dihydrolipoic acid (390 M^{-1} s^{-1}), while the lowest value (12.0 M^{-1} s^{-1}) was obtained with glutathione. Based on kinetic simulation at physiologically relevant concentrations of acceptors, thioredoxin is predicted to couple most efficiently to the MST reaction (Yadav et al. 2013).

Regulation of MST. Regulation of the MST/CAT pathway is poorly understood. Ca^{2+}-dependent regulation of MST has been reported based on the effect of varying Ca^{2+} concentrations on MST/CAT-dependent H_2S production in mouse retinal lysate (Mikami et al. 2011b). H_2S production decreased as Ca^{2+} concentration increased (0–2.9 μM) in the presence of cysteine and α-ketoglutarate (substrates for the CAT/MST pathway) but not when 3-mercaptopyruvate was used, suggesting that Ca^{2+} regulates CAT (Mikami et al. 2011b). Calmodulin is not involved in regulation of MST/CAT-dependent H_2S production (Mikami et al. 2011b). Rat MST has five cysteines and appears to be redox regulated. Of the five cysteines, three (i.e. C154, C247 & C263) are surface exposed (Nagahara and Katayama 2005; Nagahara 2012). An intersubunit disulfide bond forms between C154 and C263 under oxidizing conditions and can be reduced by thioredoxin. Thioredoxin-reduced MST is ~4.6-fold more active than the oxidized form of MST, while pretreatment of MST with DTT results in lower activation (~2.3-fold) (Nagahara et al. 2007). Human MST is a monomer and the cysteine residues that form the intersubunit disulfide in rMST are not conserved in hMST (Yadav et al. 2013). The active site cysteine (i.e. C247 in rMST) acts as another redox-sensitive switch with the potential to regulate MST (Nagahara and Katayama 2005), Treatment of rMST with stoichiometric oxidants (H_2O_2 or tetrathionate) results in inhibition due to formation of cysteine sulfenate at the active site, which can be reversed by reductants such as DTT or thioredoxin (Nagahara and Katayama 2005).

1.1.1.4 The Relative Contributions of CBS, CSE and MST to H_2S Production

It is not readily possible from the available kinetic data collected under varied buffer, pH and temperature conditions, to assess the relative roles of CBS, CSE and MST to H_2S production in different tissues. As a first step towards addressing this question,

Fig. 1.4 (Continued) 4JGT. (**c**) Reaction scheme for CAT/MST-dependent H_2S generation. (*1*) CAT catalyzes the transamination between cysteine and α-ketoglutarate to generate mercaptopyruvate and glutamate. (*2*) MST catalyzes the sulfur transfer from mercaptopyruvate to an active site cysteine, giving pyruvate and MST-bound persulfide. The latter reacts with thiols or thioredoxin (in the presence of NADPH and thioredoxin reductase) to generate H_2S

our laboratory has initiated kinetic studies in a limited set of tissues (murine liver, kidney and brain) at pH 7.4 and at 37 °C (Kabil et al. 2011; Vitvitsky et al. 2012). A second key piece of information that is needed to evaluate the contributions of the individual enzymes, is their concentrations in a given tissue, which can be obtained using quantitative Western blot analysis (Kabil et al. 2011). Finally, it is essential that sensitive and reliable methods for H_2S detection be used to monitor its formation at physiologically relevant substrate concentrations. Initial studies in our laboratory evaluating total H_2S production in murine tissues indicates that in the presence of 100 μM cysteine, liver exhibits the highest rate of H_2S production (484 ± 271 μmole h^{-1} kg^{-1} tissue) followed by kidney (104 ± 44 μmole h^{-1} kg^{-1} tissue at 0.5 mM cysteine) and then brain (29 ± 7 μmole h^{-1} kg^{-1} tissue) (Kabil et al. 2011). Quantitative Western blot analyses suggest that the expression level of all three H_2S-producing enzymes decreases in the following order: liver>kidney>brain (Kabil et al. 2011; Yadav and Banerjee, unpublished results).

The relative contributions of CBS and CSE to H_2S production at physiologically relevant substrates concentrations (560 μM serine, 100 μM cysteine and varying homocysteine ranging from its normal concentration (10 μM), to those seen under mild (40 μM) and severe (200 μM) hyperhomocysteinemia conditions) have been assessed. The kinetic simulations predict that CSE is the major H_2S producer and accounts for ~97 % of H_2S production in liver at 10 μM homocysteine, with the proportion only increasing under hyperhomocysteinemic conditions (Kabil et al. 2011). A comparable analysis including the contribution of MST is needed to provide a more complete picture of the quantitative significance of CBS, CSE and MST to H_2S production in different tissues. To assess the contribution of the MST/CAT pathway to cysteine-derived H_2S production, the assays need to be conducted in the presence of physiological concentrations of α-ketoglutarate needed by CAT to convert cysteine to 3-mercaptopyruvate.

1.1.2 Enzymology of H_2S Oxidation

1.1.2.1 Microbial Strategies for Sulfide Oxidation

A major reaction of the global sulfur cycle is the oxidation of hydrogen sulfide to sulfate. It is instructive to examine the variations in sulfide oxidation strategies used by microbes where the pathways are much better understood than in man. In microbes, inorganic sulfur compounds such as sulfide, sulfur globules, sulfite, thiosulfate and polythionates are oxidized to sulfate for generation of ATP.

Sulfide and Thiosulfate Oxidation by Phototrophic Bacteria. Green and purple sulfur bacteria utilize both sulfide and thiosulfate as electron donors for photoautotrophic growth (Gregersen et al. 2011; Grimm et al. 2011). Oxidation occurs in a stepwise manner with sulfide being converted initially to elemental sulfur, which is stored as sulfur globules either in the periplasm or on the surface of the outer membrane and utilized when sulfide is limiting. The two major enzymes directly involved in sulfide oxidation are SQR (Eq. 1.11) and flavocytochrome c sulfide dehydrogenase (Eq. 1.12), a heterodimeric flavoprotein comprising a glutathione

reductase-like subunit containing an FAD cofactor and a redox-active disulfide and a diheme cyctochrome c subunit (Chen et al. 1994). Flavocytochrome c sulfide dehydrogenase exists in both soluble and membrane bound forms and, like SQR, catalyzes the oxidation of sulfide to polysulfide while reducing the diheme cytochrome via FAD (Chen et al. 1994).

$$S^{2-} + \text{Ubiquinone}_{ox} \rightarrow S^0 + \text{Ubiquinone}_{red} \tag{1.11}$$

$$S^{2-} + \text{cyt c}_{ox} \rightarrow S^0 + \text{cyt c}_{red} \tag{1.12}$$

Sulfur globules are converted to sulfite via the cytoplasmic dissimilatory sulfite reductase pathway (Holkenbrink et al. 2011). The proteins common to bacteria harboring the dissimilatory sulfite reductase pathway include a siroheme or siroamide-containing sulfite reductase, a transmembrane electron transporting protein complex, a putative siroheme amidase and the product of the *dsr*C gene. In addition, a sulfurtransferase complex and an iron-sulfur cluster-containing NADH oxidoreductase, which is proposed to reduce sulfur polysulfides, are also present in some bacteria. The transmembrane complex shuttles electrons released during oxidation of H_2S to sulfite to quinones (Gregersen et al. 2011; Holkenbrink et al. 2011). Sulfite is toxic and is further oxidized to sulfate by one of two pathways. The first is direct oxidation catalyzed by sulfite oxidase (Eq. 1.13) and the second involves oxidation of sulfite to adenosine-5′-phosphosulfate and its subsequent conversion to sulfate liberating either ADP or ATP as the co-product (Eqs. 1.14 and 1.15) (Kappler and Dahl 2001).

$$SO_3^{2-} + H_2O \rightarrow SO_4^{2-} + 2e^- + 2H^+ \tag{1.13}$$

$$SO_3^{2-} + \text{AMP} \rightarrow \text{APS} + 2e^- \tag{1.14}$$

$$\text{APS} + \text{PPi (or Pi)} \rightarrow SO_4^{2-} + \text{ATP (or ADP)} \tag{1.15}$$

Thiosulfate is oxidized to sulfate by the multi-enzyme sulfur oxidizing (Sox) system (Eq. 1.16). The Sox system is widely distributed among phototrophic and sulfur oxidizing bacteria and also present in some green and purple bacteria

$$^{-}SSO_3 + 5\,H_2O \rightarrow 2SO_4^{2-} + 8e^- + 10H^+ \tag{1.16}$$

(Friedrich et al. 2001; Gregersen et al. 2011; Grimm et al. 2011). It is localized in the periplasm and comprises four proteins: SoxAX, SoxYZ, SoxB and SoxCD. In the first step, thiosulfate is oxidized to a cysteinyl S-thiosulfonate intermediate bound to SoxY, which is then hydrolyzed to sulfate by a dimanganese thiosulfohydrolase, SoxB. The remaining protein-bound sulfane sulfur is oxidized to sulfate by SoxCD, a heterotetramer containing a molybdenum cofactor-containing subunit and a diheme cytochrome c-containing subunit. Electrons released during thiosulfate oxidation are transferred to cytochromes and from there, to the electron transport

chain. Green and purple sulfur bacteria do not have a SoxCD component in their Sox system, and are unable to completely oxidize thiosulfate using the Sox system (Sakurai et al. 2010; Gregersen et al. 2011; Grimm et al. 2011). In these bacteria, the remaining sulfane sulfur in the SoxYZ complex is proposed to either be transferred to the bacterial sulfur globule pool or, to be oxidized by the dissimilatory sulfite reductase pathway to sulfite.

Sulfur Oxidation by Acidophilic Bacteria. Acidophilic bacteria such as *Acidithiobacillus ferrooxidans* and *Acidithiobacillus thiooxidans*, utilize a sulfur dioxygenase to oxidize elemental sulfur to sulfite (Eq. 1.17) (Rohwerder and Sand 2003). Thiol-containing proteins are predicted to be involved in mobilization of extracellular octameric elemental sulfur and presentation of sulfane sulfur to the

$$^{1}/_{8}\,S_8 + O_2 + H_2O \rightarrow SO_3^{2-} + 2H^+ \tag{1.17}$$

periplasmic sulfur dioxygenase, which does not accept sulfide or elemental sulfur as substrate (Rohwerder and Sand 2003). The product of this reaction, sulfite is oxidized to sulfate by sulfite oxidase. Two other enzymes, SQR and thiosulfate quinone oxidoreductase are also active in sulfur oxidation in acidophilic bacteria. SQR oxidizes sulfide to elemental sulfur which can react abiotically with sulfite to produce thiosulfate (Rohwerder and Sand 2007). Thiosulfate can be oxidized to tetrathionate by thiosulfate quinone oxidoreductase with the electrons being transferred to quinones.

Sulfur Oxidation by Archaea. Sulfur-oxidizing Achaea use a variation of the oxidation schemes discussed above. Thus, in *Acidianus ambivalens,* sulfur oxidation is initiated by sulfur oxygenase reductase a non-heme iron protein that catalyzes the disproportionation of elemental sulfur and/or polysulfide to sulfide and sulfite (Kletzin 1992; Kletzin et al. 2004; Urich et al. 2006). H_2S is oxidized by SQR to elemental sulfur, which can be utilized by sulfur oxygenase reductase setting up an energy-yielding cycle between the two enzymes and allowing the organism to maximize the energy gained from sulfur compounds (Brito et al. 2009). Sulfite can be further oxidized to sulfate by sulfite oxidase (Kletzin et al. 2004; Brito et al. 2009) or it can react with elemental sulfur to form thiosulfate, which is oxidized to tetrathionate. Alternatively, sulfite can be oxidized to sulfate via the APS pathway (Zimmermann et al. 1999).

In the next section, we review the literature on the mitochondrial sulfide oxidation pathway focusing on the enzymes, SQR, the persulfide dioxygenase (ETHE1) and rhodanese. The conversion of sulfide to sulfite and thiosulfate by this trio of enzymes most closely resembles the components of the sulfide oxidation pathway in acidophilic bacteria with the exception that polysulfide is not generated as an intermediate in the mammalian pathway. Instead, as discussed below, the persulfide product of SQR is transferred to an as yet unidentified acceptor. Sulfite is ultimately oxidized to sulfate by sulfite oxidase in mammals.

1.1.2.2 Sulfide Quinone Oxidoreductase

Structural Organization of SQR. SQR is found in the inner mitochondrial membrane (Theissen et al. 2003) in eukaryotes, which are believed to have acquired the nuclear encode gene from a mitochondrial endosymbiont (Theissen et al. 2003). SQR exists as a dimer or a trimer, with one FAD and one redox active disulfide in each monomer (Marcia et al. 2010). SQR oxidizes sulfide to a protein-bound persulfide and transfers electrons from H_2S to ubiquinone via a bound FAD, coupling sulfide oxidation to the electron transport chain (Fig. 1.1). Hence, sulfide functions as an inorganic substrate for the ATP-generating electron transfer chain (Bouillaud and Blachier 2011).

Several crystal structures of SQRs have been reported, notably from *Acidianus ambivalens* (Brito et al. 2009), *Aquifex aeolicus* (Marcia et al. 2009), and *Acidithiobacillus ferrooxidans* (Cherney et al. 2010). SQR belongs to the family of flavin disulfide reductases that includes glutathione reductase. SQR contains two Rossman fold domains and a C-terminal domain that is important for membrane binding (Fig. 1.5a). The FAD cofactor is found in the first N-terminal Rossman fold domain and can be non-covalently or covalently bound. In the latter case, a thioether linkage exists between a cysteine or a cysteine persulfide and the 8-methylene group of the isoalloxazine ring of FAD (Marcia et al. 2009). The catalytic disulfide is located on the *re* face of the FAD. A conserved glutamate residue in the active site is proposed to serve as a general base for deprotonating H_2S (Cherney et al. 2010). The ubiquinone-binding site is located on the *si* face of the FAD and the majority of residues in contact with the quinone are hydrophobic including F41, P43, G322, Y323, N353, Y411, F394 and F357 (*A. ferrooxidans* numbering) (Cherney et al. 2010). The aromatic ring of the quinone is sandwiched between the benzene rings of F394 and F357. The O2 atom of the flavin electron donor, and the O4 atom of the quinone acceptor are <3 Å apart. Residues Y411 and K391 have been proposed to transfer protons from water for protonation of the reduced quinone (Marcia et al. 2009; Cherney et al. 2010).

Catalytic Mechanism of SQR. The catalytic cycle of SQR is initiated by nucleophilic attack of the sulfide on the disulfide resulting in formation of a persulfide and a cysteine thiolate (Fig. 1.5b) (Brito et al. 2009; Marcia et al. 2009; Cherney et al. 2010, 2012; Jackson et al. 2012). The cysteine thiolate attacks the FAD cofactor forming a C4A adduct (Fig. 1.5c). Nucleophilic attack of an acceptor on the sulfane sulfur results in reformation of the active site disulfide and subsequent two-electron transfer to the FAD results in formation of $FADH_2$. Electron transfer from $FADH_2$ to ubiquinone regenerates FAD.

In bacterial SQRs, multiple rounds of electron transfer occur from sulfide to quinone without release of the persulfide at the end of each catalytic cycle (Brito et al. 2009; Marcia et al. 2009; Cherney et al. 2010; Jackson et al. 2012). Instead, the catalytic cycle repeats until the maximum length of the polysulfide product that can be accommodated in the active site is obtained at which point two consecutive nucleophilic attacks by the sulfide results in product release and reformation of the active site disulfide. Snapshots of these polysulfide species have been observed in structures of prokaryotic SQRs. The structure of *A. ambivalens* SQR revealed a

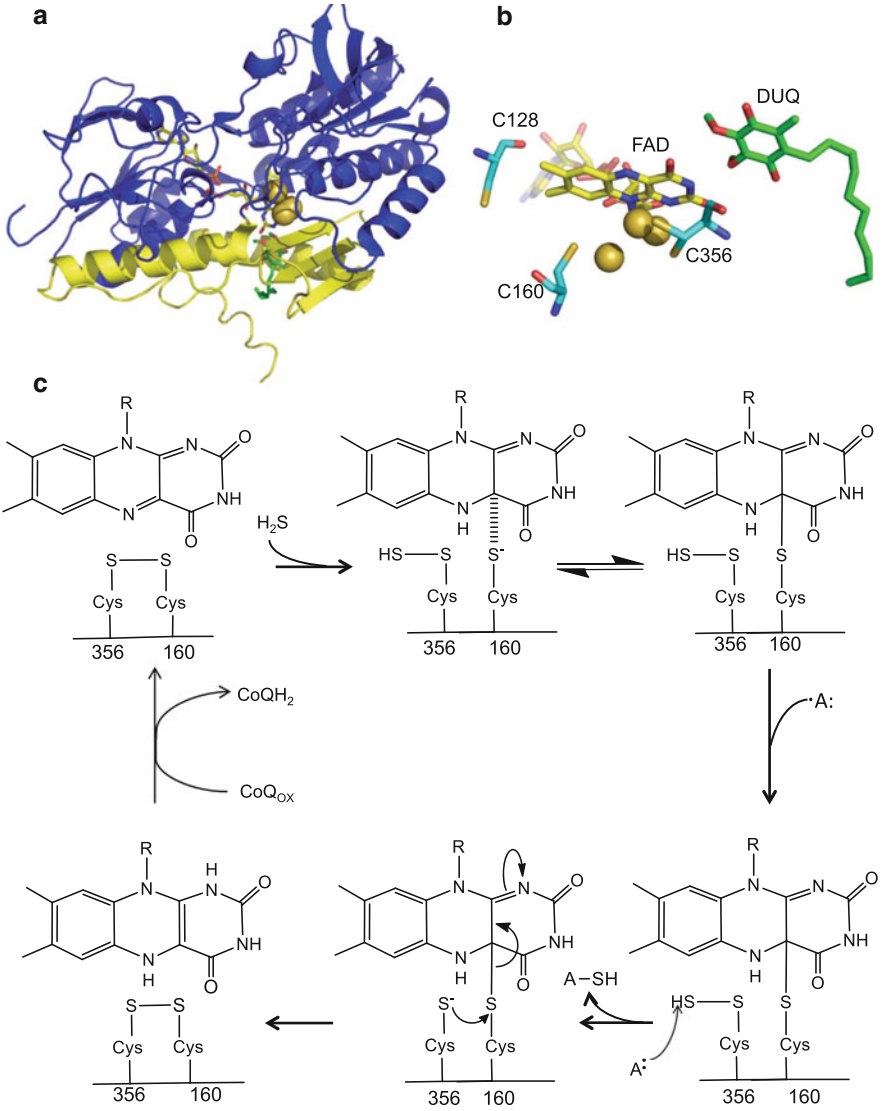

Fig. 1.5 Structure and reaction mechanism of SQR. (**a**) Structure of *A. ferrooxidans* SQR monomer displaying the N-terminal Rossman fold domains (*blue*) and the C-terminal membrane binding domain (*yellow*) and the cofactors, FAD (*yellow*) and DUQ (*green*). Active site sulfurs are shown as gold spheres (**b**) Close-up of the *A. ferrooxidans* SQR active site viewing the *re* face of the FAD isoalloxazine ring and decylubiquinone (*DUQ*) on the *si* face of FAD. Sulfur atoms between the active site cysteine residues are shown as *gold spheres*. Figure 1.5a, b were generated using PDB file 3T31. (**c**) Proposed mechanism of SQR. Reaction of H_2S reduces with the active site disulfide bond results in the formation of a persulfide on one cysteine and a covalent linkage between the other cysteine and FAD. The cysteine bound persulfide is released from the enzyme by an acceptor molecule. Reformation of the active site disulfide results in reduction of FAD to $FADH_2$. Electrons are then transferred from $FADH_2$ to ubiquinone allowing for regeneration of the oxidized active site

trisulfide bridge between the two active site cysteines (Brito et al. 2009), while the *A. ferrooxidans* structure revealed a branched intermediate between the two cysteine residues consisting of five sulfur atoms (Cherney et al. 2010, 2012). In the *A. aeolicus* SQR structures, both linear and cyclic polysulfur intermediates were observed (Marcia et al. 2009). The released product can be soluble polysulfide containing up to ten sulfur atoms (Griesbeck et al. 2002) or an octasulfur ring (Marcia et al. 2009).

In contrast, in mammalian SQRs, the persulfide product is transferred to an acceptor at the end of each catalytic cycle. Although several molecules have been proposed as acceptors of the persulfide product including sulfite and glutathione, the identity of the physiological co-substrate is not known (Jackson et al. 2012). Human SQR utilizes cyanide and sulfite as persulfide acceptors and exhibits k_{cat} values of 82 $\pm$ 6 s^{-1} and 251 $\pm$ 9 s^{-1} in the presence of 1 mM cyanide and 600 μM sulfite respectively (Jackson et al. 2012). In contrast, the k_{cat} in the presence of 1 mM glutathione as an acceptor is 19 $\pm$ 3 s^{-1}, which is reportedly identical to the background rate constant observed in the absence of an additional acceptor (k_{cat} = 18.5 $\pm$ 0.9 s^{-1}). The activity of SQR in the absence of an exogenous acceptor was attributed to sulfide acting as an acceptor for the SQR product resulting in formation of hydrogen disulfide (Jackson et al. 2012). It is not known whether ETHE1 can directly accept the persulfide product from SQR.

1.1.2.3 Persulfide Dioxygenase (ETHE1)

ETHE1, a persulfide dioxygenase, is a soluble, mitochondrial matrix enzyme that catalyzes the oxidation of glutathione persulfide to sulfite (Hildebrandt and Grieshaber 2008; Tiranti et al. 2009; Kabil and Banerjee 2012). However, the physiological substrate is not known unequivocally. Persulfide dioxygenase contains a mononuclear non-heme iron in its active site (McCoy et al. 2006; Holdorf et al. 2008). Mutations in persulfide dioxygenase result in ethylmalonic encephalopathy, an autosomal recessive disorder that results in developmental delay hemorrhagic diarrhea, acrocyanosis, petechiae, and progressive neurological failure (Tiranti et al. 2004, 2009; Mineri et al. 2008). The clinical profile of ethylmalonic encephalopathy includes high levels of lactate, high C5 and C4 acylcarnitine levels in blood, increased ethylmalonic acid concentrations in urine and cytochrome c oxidase deficiency in muscle and brain (Burlina et al. 1991; Garcia-Silva et al. 1994; Tiranti et al. 2009). Persulfide dioxygenase deficiency leads to accumulation of thiosulfate and sulfide with the latter inhibiting cytochrome *c* oxidase and possibly other enzymes and accounting in part for the observed pathology (Di Meo et al. 2011).

Both glutathione persulfide (GSSH) and CoA persulfide (CoA-SSH) serve as substrates for human persulfide dioxygenase while cysteine persulfide, glutathione and thiosulfate do not (Kabil and Banerjee 2012). However, the specific activity of the enzyme with CoA-SSH is ~50-fold lower than with GSSH. Interestingly, 5 mM glutathione, a high but physiologically relevant concentration, increases the catalytic efficiency of the persulfide dioxygenase ~3-fold. Despite the similarity between persulfide dioxygenase and glyoxylase II, the former is unable to

hydrolyze S-D-lactoylglutathione and other glutathione thioesters like glyoxylase II (Holdorf et al. 2008). This is most likely due to a C-terminal loop covering much of the active site in the dioxygenase making it smaller than the glyoxylase II active site (McCoy et al. 2006; Holdorf et al. 2008).

Structural Organization of Persulfide Dioxygenase. The structure of the *Arabidopsis thaliana* persulfide dioxygenase (McCoy et al. 2006) has been used to model the structure of the human enzyme (Fig. 1.6a) (Kabil and Banerjee 2012). The two proteins share 54 % identity. However, while the *Arabidopsis* persulfide dioxygenase is a dimer, as revealed by gel-filtration chromatography and crystallography (McCoy et al. 2006), the human enzyme is a monomer (Kabil and Banerjee 2012). The *Arabidopsis* persulfide dioxygenase has a typical metallo-β-lactamase fold containing two central β-sheets enclosed by three helices on each side. The active site iron is ligated via two histidine and one aspartate residue, which correspond to H84, H135 and D154 in the human sequence (Fig. 1.6b). The three remaining coordination sites are occupied by water resulting in octahedral coordination, typical for ferrous iron (McCoy et al. 2006; Holdorf et al. 2008).

The geometry of the iron site in persulfide dioxygenase resembles that of the 2-His-1-carboxylate facial triad family of oxygenases (Hegg and Que 1997), a common structural motif that binds mononuclear non-heme Fe^{2+}. The three coordination sites occupied by water are available for binding ligands such as O_2, substrates and/or cofactors, and allow the enzymes to tune the reactivity of the iron center (Koehntop et al. 2005; Bruijnincx et al. 2008). With three coordination sites occupied by solvent, the metal center is not reactive towards dioxygen. Substrate binding displaces solvent molecules and results in formation of a five-coordinate metal center. Replacement of neutral solvent molecules with an anionic ligand can decrease the Fe(III)/Fe(II) redox potential rendering the iron center more susceptible to oxidation by dioxygen (Koehntop et al. 2005). Hence, substrate binding primes the iron center for dioxygen binding and protects the enzyme from auto-inactivation (Koehntop et al. 2005).

The substrate-binding site is predicted to comprise residues M226, R163, Y197 and F166 in the human sequence based on structural alignment with the active site of glyoxylase II, which provides insights into how the glutathione persulfide might interacts with persulfide dioxygenase. The glyoxylase II residues Y145 and K143 are engaged in hydrogen bonds with the glutamate portion of glutathione and Y175 forms a hydrogen bond with the cysteine portion of glutathione (McCoy et al. 2006). The corresponding residues in human persulfide dioxygenase are F166, R163 and Y197. R163 is predicted to be positioned similarly to K143 and to interact with the glutamate portion of the GSSH substrate. In contrast, F166, which replaces Y145 in the persulfide dioxygenase structure, is not expected to engage in a hydrogen bonding interaction with the substrate. Y197 like Y175 in the *A. thaliana* protein, might interact with the cysteine portion of GSSH, while the sulfane sulfur of GSSH would be coordinated to the iron center (Kabil and Banerjee 2012).

Catalytic Mechanism of Persulfide Dioxygenase. Kinetic characterization of human persulfide dioxygenase and two variants mimicking missense mutations described in ethylmalonic aciduria patients, T151I and D196N, has been described

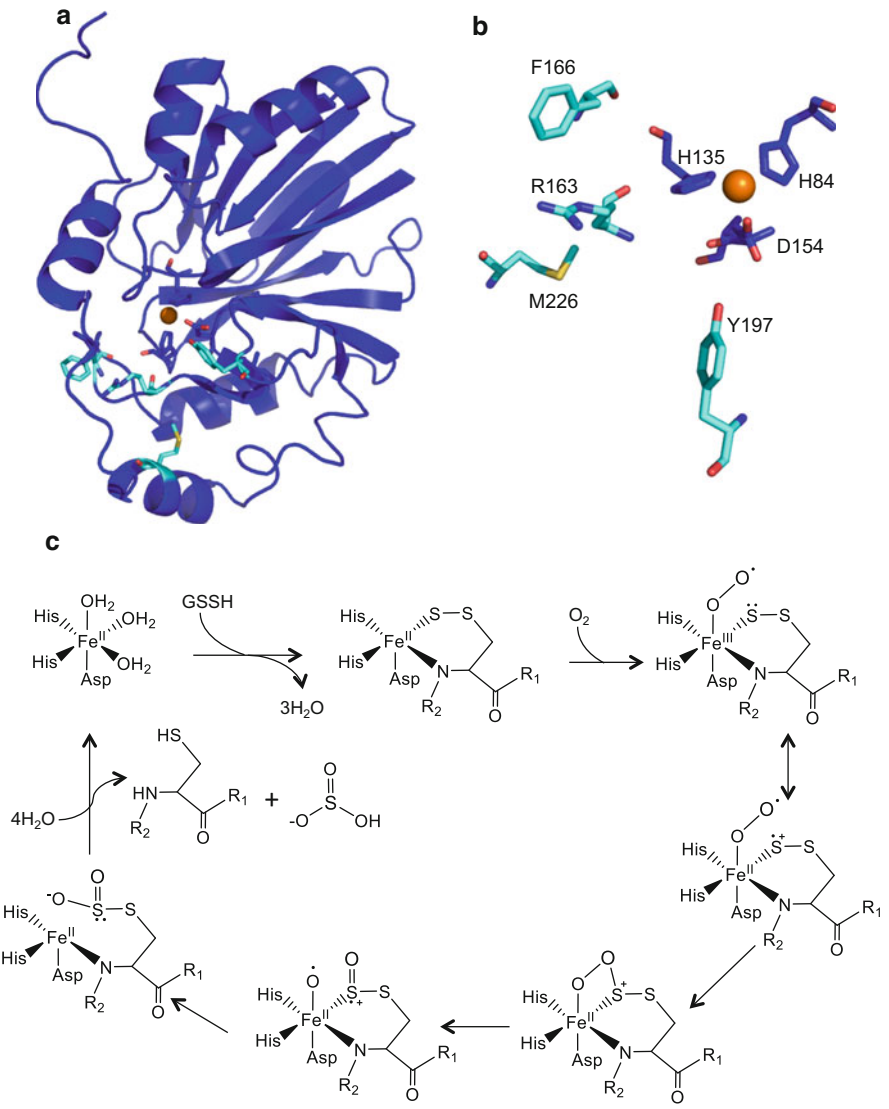

Fig. 1.6 Structure and catalytic mechanism of persulfide dioxygenase. (**a**) Structure of *A. thaliana* persulfide dioxygenase monomer. The mononuclear non-heme iron is shown in *orange* and active site residues are shown in *cyan*. (**b**) Close up of the active site of *A. thaliana* persulfide dioxygenase. The mononuclear non-heme iron is coordinated by the 2His-1Asp facial triad residues (*blue*) and other active site residues (*cyan*). Figure 1.6a, b were generated using PDB file 2GCU. (**c**) Proposed catalytic mechanism of persulfide dioxygenase for sulfite generation. Binding of the GSSH substrate displaces coordinated water and promotes binding of oxygen to the iron center to form the Fe (III) superoxo intermediate. Resonance allows for partial radical cation character of the coordinated sulfur leading to recombination and formation of a cyclic peroxo-intermediate. Cleavage of the O-O bond results in a sulfoxy-cation and an iron-bound activated oxygen atom which is transferred to the sulfur to sulfoxy-cation. Subsequent hydrolysis yields sulfite, and GSH is displaced from the active site upon water binding to the metal center. R_1 and R_2 represent residues glutamate and glycine in the GSSH substrate

(Kabil and Banerjee 2012). In the presence of GSSH, the V_{max} for human persulfide dioxygenase is 113 ± 4 μmol min^{-1} mg^{-1} protein, which corresponds to a k_{cat} of 47 s^{-1}at 22 °C. Glutathione (5 mM) decreases the K_M for GSSH ~1.4 fold and increases k_{cat} an ~2.2-fold yielding an ~3-fold increase in k_{cat}/K_M. The physiological relevance of modulation of the persulfide dioxygenase activity by GSH is not known. The T152I mutant does not affect the K_M for GSSH while the k_{cat} is diminished ~4-fold and correlates with an ~2.5 fold lower iron content compared to wild-type enzyme. T152 is located on the same loop as D154, a predicted iron ligand and participates in a hydrogen bonding interaction with the backbone of L156, which may be necessary for correct positioning of D154. The T152I mutation would result in loss of the interaction with L156 possibly leading to repositioning of D154 (Kabil and Banerjee 2012).

The impact of the D196N mutation is to increase the K_M for GSSH ~2-fold while leaving the k_{cat} unaltered. D196 is located on an internal loop distal from the active site and is proposed to hydrogen bond with F200 and H198 to stabilize the loop. The D196N mutation likely destabilizes this loop. Several other pathogenic missense mutations have been described in human persulfide dioxygenase and include Y38C, L55P, T136A, R163Q, R163W, C161Y, T164K and L185R (Tiranti et al. 2004, 2006; Mineri et al. 2008). Many of these mutations are predicted to be located near the active site and may disrupt metal or substrate binding and/or destabilize the enzyme.

The reaction mechanism proposed for persulfide dioxygenase is adapted from that described for cysteine dioxygenase (McCoy et al. 2006) and is also based on the general reaction mechanism of mononuclear non-heme iron oxygenases (Koehntop et al. 2005; Bruijnincx et al. 2008). In the proposed mechanism (Kabil and Banerjee 2012), solvent is displaced from the iron upon GSSH binding (Fig. 1.6c). The sulfane sulfur and a nitrogen atom from GSSH coordinate to the iron center resulting in a five-coordinate iron species, which is primed for O_2 binding. Binding of O_2 results in formation of a Fe (III) superoxo intermediate in which the coordinated sulfur acquires a partial radical cation character via resonance. Recombination of the Fe(III) superoxo species with the coordinated sulfur atom leads to formation of a cyclic peroxo-intermediate and is followed by homolytic cleavage of the O-O bond resulting in a sulfoxy-cation species and a metal-bound activated oxygen atom. Transfer of the activated oxygen to the sulfur and hydrolysis yields sulfite. Finally, release of GSH followed by rebinding of solvent to the active site completes the catalytic cycle (Kabil and Banerjee 2012).

1.1.2.4 Rhodanese

Rhodanese is a widely distributed protein found in Archaea, bacteria and eukaryotes (Cipollone et al. 2007). It is a mitochondrial matrix protein that catalyzes the transfer of a sulfur atom from a sulfur donor to an acceptor (Eqs. 1.18 and 1.19). Despite extensive studies on rhodanese, its precise physiological function is still not known. Historically, rhodanese was thought to be involved in

$$SO_3^{2-} + RSSH \rightarrow S_2O_3^{2-} + RSH \tag{1.18}$$

$$S_2O_3^{2-} + CN^- \rightarrow SO_3^{2-} + SCN^- \quad (1.19)$$

cyanide detoxification due to its ability to convert cyanide and thiosulfate to thiocyanate (Westley 1973; Cipollone et al. 2007). In fact, thiosulfate along with sodium nitrite is administered to treat acute cyanide poisoning. Cells that are routinely exposed to gaseous and dietary intake of cyanide, such as the epithelial cells surrounding bronchioles, hepatocytes that are proximal to the liver's blood supply and proximal tubule cells in kidney, have the highest rhodanese levels (Sylvester and Sander 1990). However, the activity of rhodanese is confined to the mitochondrial matrix, where thiosulfate enters with low efficiency suggesting that a different sulfur source than thiosulfate might be used for clearing cyanide (Westley et al. 1983). Alternatively, rhodanese might play a role in sulfur metabolism (Westley et al. 1983; Hildebrandt and Grieshaber 2008), particularly for mitochondrial thiosulfate production by transfer of the sulfane sulfur from a donor to sulfite (Hildebrandt and Grieshaber 2008).

Structural Organization of Rhodanese. Bovine liver rhodanese, which shares 89 % sequence identity with the human enzyme, has been characterized extensively. This protein is folded into two globular domains of equal size, with each containing a five stranded parallel β-sheet enclosed by two α-helices on one side and three α-helices on the other (Fig. 1.7a) (Hol et al. 1983). While both domains have a similar fold, the sequence homology is low with only 16 % sequence identity between them. The N-terminal domain is inactive due to replacement of the catalytic cysteine residue with an aspartate and plays a role in forming the active site. The catalytic C247 residue in bovine liver rhodanese is located at the bottom of a pocket formed between the two domains. The walls of the pocket comprise hydrophobic and hydrophilic regions (Fig. 1.7b). The hydrophobic regions consists of residues F212, F106, Y107, W35, and V251, and the hydrophilic region comprise residues D180, S181, R182, R186, E193, R248, K249, and T252. The persulfide intermediate is stabilized by hydrogen bonds from the backbone amides of R248, K249, V251 and the hydroxyl group of T252. Residues R186 and K249 located at the entrance of the active site pocket and their side chains are positioned to participate in binding and positioning of thiosulfate through ionic interactions and to polarize the sulfane sulfur for nucleophilic attack by the C247 thiol. It is possible that the hydrophobic region lining the active site is important for binding other substrates that contain aromatic or hydrophobic residues (Hol et al. 1983).

Catalytic Mechanism of Rhodanese. The sulfurtransferase reaction catalyzed by rhodanese occurs via a double displacement mechanism and involves formation of a stable persulfide intermediate (Hol et al. 1983; Cipollone et al. 2007a). The reaction is initiated by the nucleophilic attack of the C247 thiolate on the sulfane sulfur of thiosulfate resulting in formation of an enzyme-bound persulfide intermediate (Fig. 1.7c). Next, sulfite is released and followed by binding of a sulfur acceptor, which attacks the sulfane sulfur of the persulfide intermediate. In the case of cyanide, the product of this sulfur transfer reaction is thiocyanate (Hol et al. 1983). Release of thiocyanate completes the catalytic cycle.

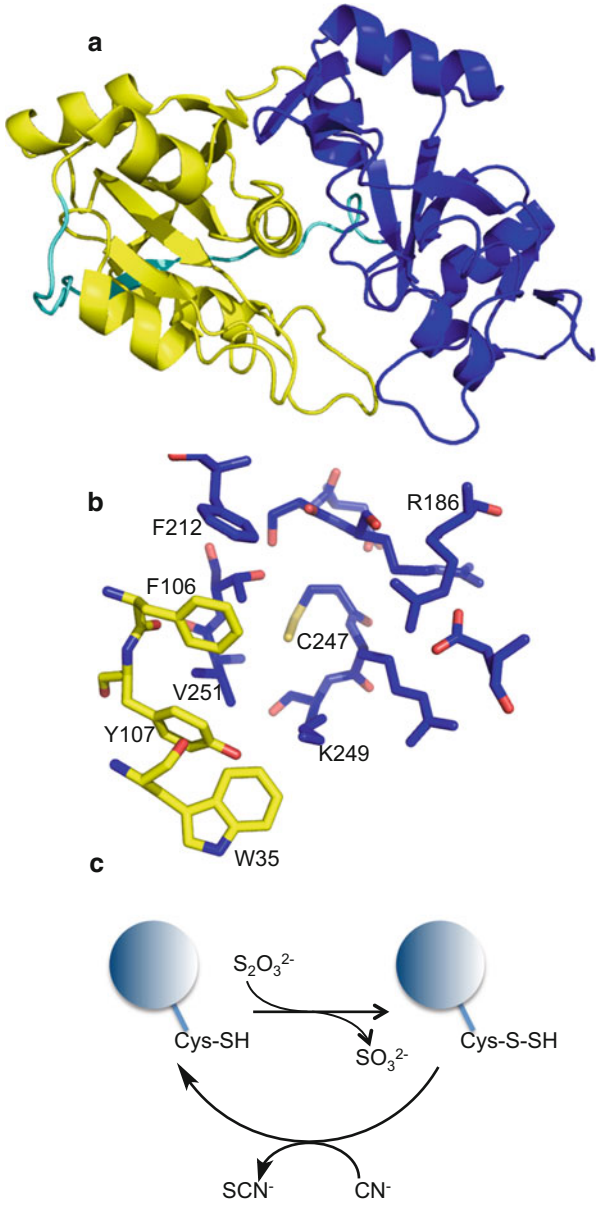

Fig. 1.7 Structure and reaction mechanism of rhodanese. (**a**) Structure of *Bos taurus* rhodanese. The protein comprises two equal sized N-terminal (*yellow*) and C-terminal (*blue*) globular domains. The linker region between the two domains is shown in *cyan*. (**b**) Close up of the rhodanese active site. The active site is located at the interface of the two domains. N- and C-terminal domain residues contribute to a hydrophobic patch (*yellow* and *blue*), while C-terminal domain residues contribute to a hydrophilic region (*blue*). Figure 1.7a, b were generated using PDB file 1RHD. (**c**) Catalytic mechanism of rhodanese for thiocyanate generation from thiosulfate. Rhodanese catalyzes the sulfur transfer from thiosulfate to an active site cysteine, resulting in sulfite and a rhodanese-bound persulfide intermediate. The latter reacts with a sulfur acceptor, in this example cyanide, to generate thiocyanate

Rhodanese also displays sulfurtransferase activity between a persulfide donor and sulfite acceptor (Eq. 1.18). The K_M values for cyanide and thiosulfate for bovine rhodanese are 0.087 ± 0.009 mM and 16.2 ± 1.6 mM, respectively (Hildebrandt and Grieshaber 2008). Similar values have also been reported for rat and lugworm rhodanese (Hildebrandt and Grieshaber 2008). In contrast, the K_Ms

for GSSH and sulfite are considerably lower (61.3 ± 17.8 μM and 21.8 ± 3.6 μM respectively), suggesting that the persulfide transferase activity of rhodanese might be more relevant physiologically than cyanide detoxification.

1.1.2.5 Mitochondrial Sulfide Oxidation: Unanswered Questions

Endogenously produced H_2S must be regulated to maintain low intracellular concentrations. In mammals, steady-state levels of H_2S are governed by flux through the synthetic pathways (transsulfuration and CAT/MST) and the sulfide oxidation pathway (Vitvitsky et al. 2012). In some prokaryotes, sulfide oxidation is essential for ATP generation. Similarly, low concentrations of H_2S (0.1–1 μM), can stimulate mammalian mitochondrial ATP production and serve as an inorganic source of ATP (Goubern et al. 2007; Bouillaud and Blachier 2011; Modis et al. 2013). An important unanswered question regarding the sulfide oxidation pathway is its organization. Since SQR oxidizes sulfide, it is reasonable to propose that it catalyzes the first step in the pathway. The ambiguity arises thereafter since the persulfide acceptor of SQR is not known. Both persulfide dioxygenase and rhodanese can oxidize persulfide forming either sulfite or thiosulfate, respectively. However, the co-substrate for rhodanese is sulfite, which is derived from the persulfide dioxygenase-catalyzed reaction. This dependence of rhodanese on the product of the dioxygenase suggests that oxidation of H_2S proceeds through SQR, the dioxygenase and then rhodanese. The products of this pathway thus configured are thiosulfate and sulfate, which is derived by oxidation of sulfite catalyzed by sulfite oxidase. The presence of two routes for sulfite oxidation in the mitochondria is paralleled in microbes where multiple sulfite oxidation routes co-exist in the same organism, e.g. the oxidation of sulfite by sulfite oxidase or via the adenosine-5′-phosphosulfate reductase pathway (Kappler and Dahl 2001).

Variants of persulfide dioxygenase fused to a rhodanese domain are found in certain bacteria (Tiranti et al. 2009). The occurrence of fused persulfide dioxygenase/rhodanese variants suggests that their proximity enhances utilization of sulfite produced by one active site and consumed by the other. However, this order of the pathway is brought into question by clinical data on ETHE1 deficient patients and ETHE1 knockout mice in which sulfite levels are greatly diminished, as expected, but thiosulfate and H_2S levels are elevated (Tiranti et al. 2009). Elevated thiosulfate in the absence of persulfide dioxygenase activity suggests that an alternative route for sulfite synthesis exists, which supports production of thiosulfate by rhodanese (Kabil and Banerjee 2012). One branch of the cysteine catabolic pathway is initiated by cysteine dioxygenase that oxidizes cysteine to cysteinesulfinate, which is further metabolized to 3-sulfinylpyruvate by CAT. 3-sulfinylpyruvate is unstable and decomposes to form pyruvate and sulfite. We have posited that the persulfide product of SQR is preferentially utilized by rhodanese under conditions of persulfide dioxygenase deficiency, explaining the observed accumulation of thiosulfate under these conditions (Kabil and Banerjee 2012). However, while cysteine catabolism is up regulated under conditions of cysteine excess (Stipanuk et al. 2004), it is unclear how this pathway responds to

persulfide dioxygenase deficiency and its role in sulfite production under these conditions warrants investigation.

In this context, understanding the fate of the persulfide product of SQR is pertinent. Bacterial polysulfide products of SQR are stored in sulfur globules until further oxidation to sulfate. However, sulfur globules have not been reported in higher organisms and in fact, eukaryotic lugworm, rat, and human SQRs require a persulfide acceptor for catalytic turnover under in vitro conditions (Hildebrandt and Grieshaber 2008; Jackson et al. 2012). The persulfide product bound to the SQR active site might be either oxidized directly by persulfide dioxygenase or rhodanese or transferred to a small molecule carrier such as GSH with the resulting GSSH serving as substrate for the persulfide dioxygenase and rhodanese. Sulfane sulfur acceptors that support the activity of SQR include sulfite, cyanide, sulfide and glutathione. Human SQR has been proposed to utilize sulfite as the physiological acceptor since it displays a 4- or 13-fold higher catalytic efficiency in the presence of either cyanide or sulfite versus glutathione (Jackson et al. 2012). Based on these results, it has been proposed that sulfite is the physiological acceptor of SQR's persulfide product resulting in the formation of thiosulfate (Jackson et al. 2012). The product of persulfide transfer to sulfite is thiosulfate, which is however not a substrate for persulfide dioxygenase (Kabil and Banerjee 2012). Of the persulfide donors that have been tested as substrates for persulfide dioxygenase only CoA-SSH exhibits activity in addition to GSSH (Kabil and Banerjee 2012). Hence, the mechanism by which the persulfide product of SQR is transferred to the persulfide dioxygenase and rhodanese is an important unanswered question in the field.

References

Agarwal N, Banerjee R (2008) Human polycomb 2 protein is a SUMO E3 ligase and alleviates substrate-induced inhibition of cystathionine β-synthase sumoylation. PLoS One 3:e4032. doi:4010.1371

Alphey MS, Williams RA, Mottram JC, Coombs GH, Hunter WN (2003) The crystal structure of Leishmania major 3-mercaptopyruvate sulfurtransferase. A three-domain architecture with a serine protease-like triad at the active site. J Biol Chem 278(48):48219–48227

Banerjee R, Evande R, Kabil O, Ojha S, Taoka S (2003) Reaction mechanism and regulation of cystathionine beta-synthase. Biochim Biophys Acta 1647(1–2):30–35

Bateman A (1997) The structure of a domain common to archaebacteria and the homocystinuria disease protein. Trends Biochem Sci 22:12–13

Bouillaud F, Blachier F (2011) Mitochondria and sulfide: a very old story of poisoning, feeding and signaling? Antioxid Redox Signal 15:379–391

Brito JA, Sousa FL, Stelter M, Bandeiras TM, Vonrhein C, Teixeira M, Pereira MM, Archer M (2009) Structural and functional insights into sulfide:quinone oxidoreductase. Biochemistry 48(24):5613–5622

Bruijnincx PC, van Koten G, Klein Gebbink RJ (2008) Mononuclear non-heme iron enzymes with the 2-His-1-carboxylate facial triad: recent developments in enzymology and modeling studies. Chem Soc Rev 37(12):2716–2744

Burlina A, Zacchello F, Dionisi-Vici C, Bertini E, Sabetta G, Bennet MJ, Hale DE, Schmidt-Sommerfeld E, Rinaldo P (1991) New clinical phenotype of branched-chain acyl-CoA oxidation defect. Lancet 338(8781):1522–1523

Carballal S, Madzelan P, Zinola CF, Grana M, Radi R, Banerjee R, Alvarez B (2008) Dioxygen reactivity and heme redox potential of truncated human cystathionine beta-synthase. Biochemistry 47(10):3194–3201

Chen ZW, Koh M, Van Driessche G, Van Beeumen JJ, Bartsch RG, Meyer TE, Cusanovich MA, Mathews FS (1994) The structure of flavocytochrome c sulfide dehydrogenase from a purple phototrophic bacterium. Science 266(5184):430–432

Chen X, Jhee KH, Kruger WD (2004) Production of the neuromodulator H_2S by cystathionine beta-synthase via the condensation of cysteine and homocysteine. J Biol Chem 279(50):52082–52086

Cherney MM, Zhang Y, Solomonson M, Weiner JH, James MN (2010) Crystal structure of sulfide: quinone oxidoreductase from Acidithiobacillus ferrooxidans: insights into sulfidotrophic respiration and detoxification. J Mol Biol 398(2):292–305

Cherney MM, Zhang Y, James MN, Weiner JH (2012) Structure-activity characterization of sulfide:quinone oxidoreductase variants. J Struct Biol 178(3):319–328

Chiku T, Padovani D, Zhu W, Singh S, Vitvitsky V, Banerjee R (2009) H_2S biogenesis by cystathionine gamma-lyase leads to the novel sulfur metabolites, lanthionine and homolanthionine, and is responsive to the grade of hyperhomocysteinemia. J Biol Chem 284:11601–11612

Cipollone R, Ascenzi P, Visca P (2007a) Common themes and variations in the rhodanese superfamily. IUBMB Life 59(2):51–59

Cipollone R, Frangipani E, Tiburzi F, Imperi F, Ascenzi P, Visca P (2007b) Involvement of Pseudomonas aeruginosa rhodanese in protection from cyanide toxicity. Appl Environ Microbiol 73(2):390–398

Crawhall JC, Parker R, Sneddon W, Young EP, Ampola MG, Efron ML, Bixby EM (1968) Beta mercaptolactate-cysteine disulfide: analog of cystine in the urine of a mentally retarded patient. Science 160(826):419–420

Di Meo I, Fagiolari G, Prelle A, Viscomi C, Zeviani M, Tiranti V (2011) Chronic exposure to sulfide causes accelerated degradation of cytochrome c oxidase in ethylmalonic encephalopathy. Antioxid Redox Signal 15(2):353–362

Evande R, Boers GHJ, Blom HJ, Banerjee R (2002) Alleviation of intrasteric inhibition by the pathogenic activation domain mutation, D444N, in human cystathionine beta-synthase. Biochemistry 41:11832–11837

Evande R, Ojha S, Banerjee R (2004) Visualization of PLP-bound intermediates in hemeless variants of human cystathionine beta-synthase: evidence that lysine 119 is a general base. Arch Biochem Biophys 427(2):188–196

Finkelstein JD, Kyle WE, Martin JL, Pick AM (1975) Activation of cystathionine synthase by adenosylmethionine and adenosylethionine. Biochem Biophys Res Commun 66(1):81–87

Friedrich CG, Rother D, Bardischewsky F, Quentmeier A, Fischer J (2001) Oxidation of reduced inorganic sulfur compounds by bacteria: emergence of a common mechanism? Appl Environ Microbiol 67(7):2873–2882

Furne J, Saeed A, Levitt MD (2008) Whole tissue hydrogen sulfide concentrations are orders of magnitude lower than presently accepted values. Am J Physiol Regul Integr Comp Physiol 295(5):R1479–R1485

Garcia-Silva MT, Campos Y, Ribes A, Briones P, Cabello A, Santos Borbujo J, Arenas J, Garavaglia B (1994) Encephalopathy, petechiae, and acrocyanosis with ethylmalonic aciduria associated with muscle cytochrome c oxidase deficiency. J Pediatr 125(5 Pt 1):843–844

Goubern M, Andriamihaja M, Nubel T, Blachier F, Bouillaud F (2007) Sulfide, the first inorganic substrate for human cells. FASEB J 21(8):1699–1706

Green EL, Taoka S, Banerjee R, Loehr TM (2001) Resonance raman characterization of the heme cofactor in cystathionine beta-synthase. Identification of the Fe-S(Cys) vibration in the six-coordinate low-spin heme. Biochemistry 40(2):459–463

Gregersen LH, Bryant DA, Frigaard NU (2011) Mechanisms and evolution of oxidative sulfur metabolism in green sulfur bacteria. Front Microbiol 2:116

Griesbeck C, Schutz M, Schodl T, Bathe S, Nausch L, Mederer N, Vielreicher M, Hauska G (2002) Mechanism of sulfide-quinone reductase investigated using site-directed mutagenesis and sulfur analysis. Biochemistry 41(39):11552–11565

Grimm F, Franz B, Dahl C (2011) Regulation of dissimilatory sulfur oxidation in the purple sulfur bacterium allochromatium vinosum. Front Microbiol 2:51

Hegg EL, Que L Jr (1997) The 2-His-1-carboxylate facial triad–an emerging structural motif in mononuclear non-heme iron(II) enzymes. Eur J Biochem 250(3):625–629

Hildebrandt TM, Grieshaber MK (2008) Three enzymatic activities catalyze the oxidation of sulfide to thiosulfate in mammalian and invertebrate mitochondria. FEBS J 275(13):3352–3361

Hol WG, Lijk LJ, Kalk KH (1983) The high resolution three-dimensional structure of bovine liver rhodanese. Fundam Appl Toxicol 3(5):370–376

Holdorf MM, Bennett B, Crowder MW, Makaroff CA (2008) Spectroscopic studies on Arabidopsis ETHE1, a glyoxalase II-like protein. J Inorg Biochem 102(9):1825–1830

Holkenbrink C, Barbas SO, Mellerup A, Otaki H, Frigaard NU (2011) Sulfur globule oxidation in green sulfur bacteria is dependent on the dissimilatory sulfite reductase system. Microbiology 157(Pt 4):1229–1239

Huang S, Chua JH, Yew WS, Sivaraman J, Moore PK, Tan C-H, Deng L-W (2010) Site-directed mutagenesis on human cystathionine-γ-lyase reveals insights into the modulation of H_2S production. J Mol Biol 396(3):708–718

Jackson MR, Melideo SL, Jorns MS (2012) Human sulfide: quinone oxidoreductase catalyzes the first step in hydrogen sulfide metabolism and produces a sulfane sulfur metabolite. Biochemistry 51(34):6804–6815

Janosik M, Kery V, Gaustadnes M, Maclean KN, Kraus JP (2001) Regulation of human cystathionine beta-synthase by S-adenosyl-L- methionine: evidence for two catalytically active conformations involving an autoinhibitory domain in the C-terminal region. Biochemistry 40(35):10625–10633

Jarabak R, Westley J (1978) Steady-state kinetics of 3-mercaptopyruvate sulfurtransferase from bovine kidney. Arch Biochem Biophys 185(2):458–465

Jhee KH, Niks D, McPhie P, Dunn MF, Miles EW (2001) The reaction of yeast cystathionine beta-synthase is rate-limited by the conversion of aminoacrylate to cystathionine. Biochemistry 40(36):10873–10880

Kabil O, Banerjee R (2010) The redox biochemistry of hydrogen sulfide. J Biol Chem 285:21903–21907

Kabil O, Banerjee R (2012) Characterization of patient mutations in human persulfide dioxygenase (ETHE1) involved in H_2S catabolism. J Biol Chem 287:44561–44567

Kabil O, Vitvitsky V, Xie P, Banerjee R (2011a) The quantitative significance of the transsulfuration enzymes for H_2S production in murine tissues. Antioxid Redox Signal 15:363–372

Kabil O, Weeks CL, Carballal S, Gherasim C, Alvarez B, Spiro TG, Banerjee R (2011b) Reversible heme-dependent regulation of human cystathionine beta-synthase by a flavoprotein oxidoreductase. Biochemistry 50(39):8261–8263

Kappler U, Dahl C (2001) Enzymology and molecular biology of prokaryotic sulfite oxidation. FEMS Microbiol Lett 203(1):1–9

Kery V, Poneleit L, Kraus JP (1998) Trypsin cleavage of human cystathionine beta-synthase into an evolutionarily conserved active core: structural and functional consequences. Arch Biochem Biophys 355(2):222–232

Kimura H (2010) Hydrogen sulfide: from brain to gut. Antioxid Redox Signal 12(9):1111–1123

Kletzin A (1992) Molecular characterization of the sor gene, which encodes the sulfur oxygenase/reductase of the thermoacidophilic Archaeum Desulfurolobus ambivalens. J Bacteriol 174(18):5854–5859

Kletzin A, Urich T, Muller F, Bandeiras TM, Gomes CM (2004) Dissimilatory oxidation and reduction of elemental sulfur in thermophilic archaea. J Bioenerg Biomembr 36(1):77–91

Koehntop KD, Emerson JP, Que L Jr (2005) The 2-His-1-carboxylate facial triad: a versatile platform for dioxygen activation by mononuclear non-heme iron(II) enzymes. J Biol Inorg Chem 10(2):87–93

Koutmos M, Kabil O, Smith JL, Banerjee R (2010) Structural basis for substrate activation and regulation by cystathionine beta-synthase domains in cystathionine beta-synthase. Proc Natl Acad Sci USA 107:20958–20963

Kraus JP, Janosik M, Kozich V, Mandell R, Shih V, Sperandeo MP, Sebastio G, de Franchis R, Andria G, Kluijtmans LA, Blom H, Boers GH, Gordon RB, Kamoun P, Tsai MY, Kruger WD, Koch HG, Ohura T, Gaustadnes M (1999) Cystathionine beta-synthase mutations in homocystinuria. Hum Mutat 13(5):362–375

Levitt MD, Abdel-Rehim MS, Furne J (2011) Free and acid-labile hydrogen sulfide concentrations in mouse tissues: anomalously high free hydrogen sulfide in aortic tissue. Antioxid Redox Signal 15:373–378

Marcia M, Ermler U, Peng G, Michel H (2009) The structure of Aquifex aeolicus sulfide:quinone oxidoreductase, a basis to understand sulfide detoxification and respiration. Proc Natl Acad Sci USA 106(24):9625–9630

Marcia M, Ermler U, Peng G, Michel H (2010) A new structure-based classification of sulfide: quinone oxidoreductases. Proteins 78(5):1073–1083

McCoy JG, Bailey LJ, Bitto E, Bingman CA, Aceti DJ, Fox BG, Phillips GN Jr (2006a) Structure and mechanism of mouse cysteine dioxygenase. Proc Natl Acad Sci USA 103(9):3084–3089

McCoy JG, Bingman CA, Bitto E, Holdorf MM, Makaroff CA, Phillips GN Jr (2006b) Structure of an ETHE1-like protein from Arabidopsis thaliana. Acta Crystallogr D Biol Crystallogr 62(Pt 9):964–970

Meier M, Janosik M, Kery V, Kraus JP, Burkhard P (2001) Structure of human cystathionine beta-synthase: a unique pyridoxal 5′- phosphate-dependent heme protein. EMBO J 20(15):3910–3916

Meister A, Fraser PE, Tice SV (1954) Enzymatic desulfuration of beta-mercaptopyruvate to pyruvate. J Biol Chem 206(2):561–575

Messerschmidt A, Worbs M, Steegborn C, Wahl MC, Huber R, Laber B, Clausen T (2003) Determinants of enzymatic specificity in the Cys-Met-metabolism PLP-dependent enzymes family: crystal structure of cystathionine gamma-lyase from yeast and intrafamiliar structure comparison. Biol Chem 384(3):373–386

Mikami Y, Shibuya N, Kimura Y, Nagahara N, Ogasawara Y, Kimura H (2011a) Thioredoxin and dihydrolipoic acid are required for 3-mercaptopyruvate sulfurtransferase to produce hydrogen sulfide. Biochem J 439(3):479–485

Mikami Y, Shibuya N, Kimura Y, Nagahara N, Yamada M, Kimura H (2011b) Hydrogen sulfide protects the retina from light-induced degeneration by the modulation of Ca2+ influx. J Biol Chem 286(45):39379–39386

Mikami Y, Shibuya N, Ogasawara Y, Kimura H (2013) Hydrogen sulfide is produced by cystathionine gamma-lyase at the steady-state low intracellular Ca(2+) concentrations. Biochem Biophys Res Commun 431(2):131–135

Mineri R, Rimoldi M, Burlina AB, Koskull S, Perletti C, Heese B, von Dobeln U, Mereghetti P, Di Meo I, Invernizzi F, Zeviani M, Uziel G, Tiranti V (2008) Identification of new mutations in the ETHE1 gene in a cohort of 14 patients presenting with ethylmalonic encephalopathy. J Med Genet 45(7):473–478

Modis K, Coletta C, Erdelyi K, Papapetropoulos A, Szabo C (2013) Intramitochondrial hydrogen sulfide production by 3-mercaptopyruvate sulfurtransferase maintains mitochondrial electron flow and supports cellular bioenergetics. FASEB J 27(2):601–611

Mudd SH, Finkelstein JD, Irreverre F, Laster L (1964) Homocystinuria: an enzymatic defect. Science 143:1443–1445

Nagahara N (2012) Regulation of mercaptopyruvate sulfurtransferase activity via intrasubunit and intersubunit redox-sensing switches. Antioxid Redox Signal [Epub ahead of print]

Nagahara N, Katayama A (2005) Post-translational regulation of mercaptopyruvate sulfurtransferase via a low redox potential cysteine-sulfenate in the maintenance of redox homeostasis. J Biol Chem 280(41):34569–34576

Nagahara N, Nishino T (1996) Role of amino acid residues in the active site of rat liver mercaptopyruvate sulfurtransferase. J Biol Chem 271(44):27395–27401

Nagahara N, Sawada N (2006) The mercaptopyruvate pathway in cysteine catabolism: a physiologic role and related disease of the multifunctional 3-mercaptopyruvate sulfurtransferase. Curr Med Chem 13(10):1219–1230

Nagahara N, Ito T, Kitamura H, Nishino T (1998) Tissue and subcellular distribution of mercaptopyruvate sulfurtransferase in the rat: confocal laser fluorescence and immunoelectron microscopic studies combined with biochemical analysis. Histochem Cell Biol 110(3):243–250

Nagahara N, Ito T, Minami M (1999) Mercaptopyruvate sulfurtransferase as a defense against cyanide toxication: molecular properties and mode of detoxification. Histol Histopathol 14(4):1277–1286

Nagahara N, Yoshii T, Abe Y, Matsumura T (2007) Thioredoxin-dependent enzymatic activation of mercaptopyruvate sulfurtransferase. An intersubunit disulfide bond serves as a redox switch for activation. J Biol Chem 282(3):1561–1569

Ojha S, Hwang J, Kabil O, Penner-Hahn JE, Banerjee R (2000) Characterization of the heme in human cystathionine beta-synthase by X-ray absorption and electron paramagnetic resonance spectroscopies. Biochemistry 39:10542–10547

Ojha S, Wu J, LoBrutto R, Banerjee R (2002) Effects of heme ligand mutations including a pathogenic variant, H65R, on the properties of human cystathionine beta syntase. Biochemistry 41:4649–4654

Pey AL, Majtan T, Sanchez-Ruiz JM, Kraus JP (2013) Human cystathionine beta-synthase (CBS) contains two classes of binding sites for S-adenosylmethionine (SAM): complex regulation of CBS activity and stability by SAM. Biochem J 449(1):109–121

Prudova A, Bauman Z, Braun A, Vitvitsky V, Lu SC, Banerjee R (2006) S-Adenosylmethionine stabilizes cystathionine beta-synthase and modulates redox capacity. Proc Natl Acad Sci USA 103(17):6489–6494

Puranik M, Weeks CL, Lahaye D, Kabil O, Taoka S, Nielsen SB, Groves JT, Banerjee R, Spiro TG (2006) Dynamics of carbon monoxide binding to cystathionine beta-synthase. J Biol Chem 281(19):13433–13438

Quazi F, Aitken SM (2009) Characterization of the S289A, D mutants of yeast cystathionine beta-synthase. Biochim Biophys Acta-Proteins Proteomic 1794(6):892–897

Rohwerder T, Sand W (2003) The sulfane sulfur of persulfides is the actual substrate of the sulfur-oxidizing enzymes from Acidithiobacillus and Acidiphilium spp. Microbiology 149(Pt 7): 1699–1710

Rohwerder T, Sand W (2007) The sulfane sulfur of persulfides is the actual substrate of the sulfur-oxidizing enzymes from Acidithiobacillus and Acidiphilium spp. Microbiology 149:1699–1710

Sakurai H, Ogawa T, Shiga M, Inoue K (2010) Inorganic sulfur oxidizing system in green sulfur bacteria. Photosynth Res 104(2–3):163–176

Scott JW, Hawley SA, Green KA, Anis M, Stewart G, Scullion GA, Norman DG, Hardie DG (2004) CBS domains form energy-sensing modules whose binding of adenosine ligands is disrupted by disease mutations. J Clin Invest 113(2):274–284

Sen S, Banerjee R (2007) A pathogenic linked mutation in the catalytic core of human cystathionine beta-synthase disrupts allosteric regulation and allows kinetic characterization of a full-length dimer. Biochemistry 46(13):4110–4116

Shan X, Kruger WD (1998) Correction of disease-causing CBS mutations in yeast. Nat Genet 19(1):91–93

Shibuya N, Tanaka M, Yoshida M, Ogasawara Y, Togawa T, Ishii K, Kimura H (2009) 3-Mercaptopyruvate sulfurtransferase produces hydrogen sulfide and bound sulfane sulfur in the brain. Antioxid Redox Signal 11:703–714

Shibuya N, Koike S, Tanaka M, Ishigami-Yuasa M, Kimura Y, Ogasawara Y, Fukui K, Nagahara N, Kimura H (2013) A novel pathway for the production of hydrogen sulfide from D-cysteine in mammalian cells. Nat Commun 4:1366

Singh S, Banerjee R (2011) PLP-dependent H_2S biogenesis. Biochim Biophys Acta 1814:1518–1527

Singh S, Madzelan P, Banerjee R (2007) Properties of an unusual heme cofactor in PLP-dependent cystathionine beta-synthase. Nat Prod Rep 24:631–639

Singh S, Madzelan P, Stasser J, Weeks CL, Becker D, Spiro TG, Penner-Hahn J, Banerjee R (2009a) Modulation of the heme electronic structure and cystathionine beta-synthase activity by second coordination sphere ligands: the role of heme ligand switching in redox regulation. J Inorg Biochem 103:689–697

Singh S, Padovani D, Leslie RA, Chiku T, Banerjee R (2009b) Relative contributions of cystathionine beta-synthase and gamma-cystathionase to H_2S biogenesis via alternative trans-sulfuration reactions. J Biol Chem 284(33):22457–22466

Singh S, Ballou DP, Banerjee R (2011) Pre-steady-state kinetic analysis of enzyme-monitored turnover during cystathionine beta-synthase-catalyzed H_2S generation. Biochemistry 50:419–425

Spallarossa A, Forlani F, Carpen A, Armirotti A, Pagani S, Bolognesi M, Bordo D (2004) The "rhodanese" fold and catalytic mechanism of 3-mercaptopyruvate sulfurtransferases: crystal structure of SseA from Escherichia coli. J Mol Biol 335(2):583–593

Stipanuk MH, Beck PW (1982) Characterization of the enzymic capacity for cysteine desulphhydration in liver and kidney of the rat. Biochem J 206(2):267–277

Stipanuk MH, Hirschberger LL, Londono MP, Cresenzi CL, Yu AF (2004) The ubiquitin-proteasome system is responsible for cysteine-responsive regulation of cysteine dioxygenase concentration in liver. Am J Physiol Endocrinol Metab 286(3):E439–E448

Sun Q, Collins R, Huang S, Holmberg-Schiavone L, Anand GS, Tan CH, van-den Berg S, Deng LW, Moore PK, Karlberg T, Sivaraman J (2009) Structural basis for the inhibition mechanism of human cystathionine gamma-lyase, an enzyme responsible for the production of H_2S. J Biol Chem 284(5):3076–3085

Sylvester M, Sander C (1990) Immunohistochemical localization of rhodanese. Histochem J 22(4):197–200

Taoka S, Banerjee R (2001) Characterization of NO binding to human cystathionine [beta]-synthase: possible implications of the effects of CO and NO binding to the human enzyme. J Inorg Biochem 87(4):245–251

Taoka S, Banerjee R (2002) Stopped-flow kinetic analysis of the reaction catalyzed by the full length yeast cystathionine beta synthase. J Biol Chem 277:22421–22425

Taoka S, Ohja S, Shan X, Kruger WD, Banerjee R (1998) Evidence for heme-mediated redox regulation of human cystathionine beta-synthase activity. J Biol Chem 273(39):25179–25184

Taoka S, West M, Banerjee R (1999) Characterization of the heme and pyridoxal phosphate cofactors of human cystathionine β-synthase reveals nonequivalent active sites. Biochemistry 38(9):2738–2744

Taoka S, Green EL, Loehr TM, Banerjee R (2001) Mercuric chloride-induced spin or ligation state changes in ferric or ferrous human cystathionine beta-synthase inhibit enzyme activity. J Inorg Biochem 87:253–259

Taoka S, Lepore BW, Kabil O, Ojha S, Ringe D, Banerjee R (2002) Human cystathionine beta-synthase is a heme sensor protein. Evidence that the redox sensor is heme and not the vicinal cysteines in the CXXC motif seen in the crystal structure of the truncated enzyme. Biochemistry 41(33):10454–10461

Theissen U, Hoffmeister M, Grieshaber M, Martin W (2003) Single eubacterial origin of eukaryotic sulfide: quinone oxidoreductase, a mitochondrial enzyme conserved from the early evolution of eukaryotes during anoxic and sulfidic times. Mol Biol Evol 20(9):1564–1574

Tiranti V, D'Adamo P, Briem E, Ferrari G, Mineri R, Lamantea E, Mandel H, Balestri P, Garcia-Silva MT, Vollmer B, Rinaldo P, Hahn SH, Leonard J, Rahman S, Dionisi-Vici C, Garavaglia B,

Gasparini P, Zeviani M (2004) Ethylmalonic encephalopathy is caused by mutations in ETHE1, a gene encoding a mitochondrial matrix protein. Am J Hum Genet 74(2):239–252

Tiranti V, Briem E, Lamantea E, Mineri R, Papaleo E, De Gioia L, Forlani F, Rinaldo P, Dickson P, Abu-Libdeh B, Cindro-Heberle L, Owaidha M, Jack RM, Christensen E, Burlina A, Zeviani M (2006) ETHE1 mutations are specific to ethylmalonic encephalopathy. J Med Genet 43(4):340–346

Tiranti V, Viscomi C, Hildebrandt T, Di Meo I, Mineri R, Tiveron C, Levitt MD, Prelle A, Fagiolari G, Rimoldi M, Zeviani M (2009) Loss of ETHE1, a mitochondrial dioxygenase, causes fatal sulfide toxicity in ethylmalonic encephalopathy. Nat Med 15(2):200–205

Urich T, Gomes CM, Kletzin A, Frazao C (2006) X-ray structure of a self-compartmentalizing sulfur cycle metalloenzyme. Science 311(5763):996–1000

Vitvitsky V, Kabil O, Banerjee R (2012) High turnover rates for hydrogen sulfide allow for rapid regulation of its tissue concentrations. Antioxid Red Signal 17(1):22–31

Wang J, Hegele RA (2003) Genomic basis of cystathioninuria (MIM 219500) revealed by multiple mutations in cystathionine gamma-lyase (CTH). Hum Genet 112(4):404–408

Weeks CL, Singh S, Madzelan P, Banerjee R, Spiro TG (2009) Heme regulation of human cystathionine beta-synthase activity: insights from fluorescence and Raman spectroscopy. J Am Chem Soc 131(35):12809–12816

Westley J (1973) Rhodanese. Adv Enzymol Relat Areas Mol Biol 39:327–368

Westley J, Adler H, Westley L, Nishida C (1983) The sulfurtransferases. Fundam Appl Toxicol 3(5):377–382

Williams RA, Kelly SM, Mottram JC, Coombs GH (2003) 3-Mercaptopyruvate sulfurtransferase of Leishmania contains an unusual C-terminal extension and is involved in thioredoxin and antioxidant metabolism. J Biol Chem 278(3):1480–1486

Yadav PK, Banerjee R (2012) Detection of reaction intermediates during human cystathionine beta-synthase-monitored turnover and H_2S production. J Biol Chem 287:43464–43471

Yadav PK, Yamada K, Chiku T, Koutmos M, Banerjee R (2013) Structure and kinetic analysis of H_2S production by human mercaptopyruvate sulfurtransferase. J Biol Chem 288(27): 20002–20013

Yadav PK, Xie P, Banerjee R (2012) Allosteric communication between the pyridoxal 5′-phosphate (PLP) and heme sites in the H_2S generator human cystathionine beta-synthase. J Biol Chem 287(45):37611–37620

Yamagata S, Yasugahira T, Okuda Y, Iwama T (2003) Conversion of the aminocrotonate intermediate limits the rate of gamma-elimination reaction catalyzed by L-cystathionine gamma-lyase of the yeast Saccharomyces cerevisiae. J Biochem 134(4):607–613

Yamamoto T, Takano N, Ishiwata K, Suematsu M (2011) Carbon monoxide stimulates global protein methylation via its inhibitory action on cystathionine beta-synthase. J Clin Biochem Nutr 48(1):96–100

Yang G, Wu L, Jiang B, Yang W, Qi J, Cao K, Meng Q, Mustafa AK, Mu W, Zhang S, Snyder SH, Wang R (2008) H_2S as a physiologic vasorelaxant: hypertension in mice with deletion of cystathionine gamma-lyase. Science 322(5901):587–590

Zhong WX, Wang YB, Peng L, Ge XZ, Zhang J, Liu SS, Zhang XN, Xu ZH, Chen Z, Luo JH (2012) Lanthionine synthetase C-like protein 1 interacts with and inhibits cystathionine beta-synthase: a target for neuronal antioxidant defense. J Biol Chem 287(41):34189–34201

Zimmermann P, Laska S, Kletzin A (1999) Two modes of sulfite oxidation in the extremely thermophilic and acidophilic archaeon acidianus ambivalens. Arch Microbiol 172(2):76–82